Harold V Ioakes

NATIONAL ADVISORY COMMITTEE FOR AERONAUTICS

TECHNICAL NOTE

No. 1080

SUMMARY AND ANALYSIS OF DATA ON DAMPING IN YAW AND PITCH FOR A NUMBER OF AIRPLANE MODELS

By William E. Cotter, Jr.

Langley Memorial Aeronautical Laboratory
Langley Field, Va.

Washington
May 1946

NATIONAL ADVISORY COMMITTEE FOR AERONAUTICS

TECHNICAL NOTE NO. 1080

SUMMARY AND ANALYSIS OF DATA ON DAMPING IN YAW AND PITCH FOR A NUMBER OF AIRPLANE MODELS

By William E. Cotter, Jr.

SUMMARY

Damping data obtained from free-flight-tunnel tests of 13 models have been summarized and these results have been analyzed and compared with calculated results. The contributions of the wing, flaps, fuselage, tail surfaces, and power to the damping in pitch and yaw were studied. For complete models, fairly good agreement was obtained between experimental and calculated values for power-off, flaps-neutral conditions. Further research on the effects of sidewash on the damping in yaw for power-on and/or flaps-down conditions is needed. The damping provided by a wing without flaps was found to be small. Deflection of full-span flaps noticeably increased the damping in yaw. The contribution to damping of the fuselage was found to be negligible. The tail surfaces of conventional designs contributed 70 to 90 percent of the damping in yaw and pitch. Power application increased damping both in yaw and in pitch. The damping of tailless designs was about one-third to one-tenth that of conventional designs.

INTRODUCTION

Dynamic-stability calculations for an airplane require knowledge of values of the damping-in-pitch derivative C_{m_q} (the pitching-moment coefficient due to pitching velocity) and the damping-in-yaw parameter C_{n_r} (the yawing-moment coefficient due to yawing velocity). At the present time, however, very little experimental data on these derivatives for modern airplanes are available.

The damping derivatives C_{m_q} and C_{n_r} have been measured in the Langley free-flight tunnel during stability investigations as an aid in analyzing the stability characteristics of some models. These measurements are summarized herein to provide a source of experimental data, and a limited analysis of the data and a comparison with calculated results are also presented. The values of C_{n_r} and C_{m_q} were determined experimentally by the free-oscillation method described in references 1 and 2. The calculations were made by the methods of references 2 to 6.

Data are presented for a rectangular wing and for 13 complete airplane models, five of which are tailless designs. The term "tailless" refers to an airplane with no horizontal tail; however, such designs generally incorporate some type of vertical tail. The term "conventional" in this paper refers to airplanes other than tailless airplanes. Values of C_{n_r} and C_{m_q} over the normal lift range are presented in most cases. The effects of tail area, tail length, flap deflection, and power on the damping in yaw and pitch are shown.

SYMBOLS

S	wing area, square feet
b	wing span, feet
c	wing mean aerodynamic chord, feet
A	aspect ratio
λ	taper ratio. (ratio of extended tip chord to chord at plane of symmetry)
l	geometric tail length feet (longitudinal distance from center of gravity to tail center pressure); positive when measured rearward
l_e	effective tail length feet; when divided by the velocity of the airplane this distance represents time lag in growth of downwash and development of lift by tail

y lateral distance from center of gravity to vertical tail, feet

S_V vertical-tail area, square feet

S_H horizontal-tail area, square feet

V airspeed, feet per second

ρ mass density of air, slugs per cubic foot

q pitching angular velocity, radians per second

r yawing angular velocity, radians per second

α angle of attack of fuselage center line, degrees

β angle of sideslip, radians

ϵ angle of downwash at horizontal tail, degrees

i_t incidence of horizontal tail, degrees

δ_f flap deflection, degrees

x distance of aerodynamic center of the wing from axis of rotation, feet; positive rearward

D propeller diameter, feet

T_c thrust coefficient $\left(\frac{\text{Thrust}}{\rho V^2 D^2}\right)$

C_L lift coefficient $\left(\frac{\text{Lift}}{\frac{1}{2}\rho V^2 S}\right)$

C_{L_w} lift coefficient due to wing angle of attack $\left(\frac{\text{Wing lift}}{\frac{1}{2}\rho V^2 S}\right)$

ΔC_{L_f} increment of lift coefficient due to flap deflection

C_{D_o} profile-drag coefficient of wing $\left(\frac{\text{Profile drag}}{\frac{1}{2}\rho V^2 S}\right)$

ΔC_{D_t} increment of drag coefficient due to vertical tails $\left(\frac{\text{Vertical-tail drag}}{\frac{1}{2}\rho V^2 S}\right)$

$\Delta C_{D_{of}}$ increment of profile-drag coefficient due to flap deflection

C_n yawing-moment coefficient $\left(\frac{\text{Yawing moment}}{\frac{1}{2}\rho V^2 Sb}\right)$

C_m pitching-moment coefficient $\left(\frac{\text{Pitching moment}}{\frac{1}{2}\rho V^2 Sc}\right)$

$\frac{dC_L}{d\alpha}$ rate of change of airplane lift coefficient with angle of attack, per degree

C_{n_β} rate of change of yawing-moment coefficient with angle of sideslip, per radian $\left(\partial C_n / \partial \beta\right)$

$\Delta C_{n_{\beta_t}}$ increment of C_{n_β} due to vertical tail, per radian $\left[\left(\Delta \frac{\partial C_n}{\partial \beta}\right)_t\right]$

C_{n_r} rate of change of yawing-moment coefficient with yawing parameter $rb/2V$, per radian $\left(\frac{\partial C_n}{\partial \frac{rb}{2V}}\right)$

$C_{n_{r_t}}$ increment of C_{n_r} due to vertical tail, per radian $\left[\left(\Delta \frac{\partial C_n}{\partial \frac{rb}{2V}}\right)_t\right]$

$C_{m_{i_t}}$ rate of change of pitching-moment coefficient with horizontal tail incidence, per radian $\left(\frac{\partial C_m}{\partial i_t}\right)$

$C_{L_{q_{a.c.}}}$ rate of change of lift coefficient with pitching parameter $\frac{qc}{2V}$, for rotation about aerodynamic center, per radian $\left[\left(\frac{\partial C_L}{\partial \frac{qc}{2V}}\right)_{a.c.}\right]$

C_{m_q} rate of change of pitching-moment coefficient with pitching parameter $qc/2V$, referred to center of gravity, per radian $\left(\frac{\partial C_m}{\partial \frac{qc}{2V}}\right)$

$C_{m_{q_{a.c.}}}$ C_{m_q} referred to the aerodynamic center

$\Delta C_{m_{q_t}}$ increment of C_{m_q} due to horizontal tail $\left[\left(\frac{\partial C_m}{\Delta \frac{qc}{2V}}\right)_t\right]$

METHODS

Test Data

All the experimental data presented herein were obtained from tests made in the Langley free-flight tunnel, which is described in reference 7. The apparatus and testing procedure used for the damping-in-yaw tests are explained in reference 2. Similar apparatus and testing procedure were used to measure damping in pitch.

Most of the data were obtained from tests made as a part of routine investigations on specific airplane models. A few other tests were made to check existing data and to supply missing information pertinent to the present paper. Sketches of the specific models tested are shown for each model in figures 1 to 12. Flaps are shown in sketches of models that were tested with flaps deflected and propellers are included in sketches of models tested with power or with windmilling propellers. In addition, a rectangular wing of aspect ratio 6 was tested to determine C_{n_r}.

All models were mounted with the axis of rotation at the center of gravity or as near the center of gravity as was practicable for the particular model construction. All tests were made within an effective Reynolds number range from 200,000 to 300,000. The scope of the data is given in table I.

Corrections to Test Data

The damping-in-pitch parameter C_{m_q} at a constant pitching velocity for a complete model cannot be determined directly from oscillation tests (reference 8) because of the time lag between the formation of downwash at the wing and the action of the downwash on the horizontal tail. In an oscillation test, this lag of downwash causes the instantaneous effective angle of attack of the tail to be greater than it would be if the wing were not present. The damping in pitch of the tail consequently appears greater than it would in a test for which the wing and tail angles of attack remain constant (such as in tests by the whirling-arm method described in reference 8). The damping in pitch measured in an oscillation test represents the damping that the airplane would have in a rapid longitudinal oscillation having a period corresponding to that used in the test, whereas the results of the whirling-arm tests represent closely the damping of a long-period oscillation or phugoid motion. The following formula (derived from a similar formula from reference 8) was used to correct the damping measured in an oscillation test for the increase in tail angle of attack due to the effects of lag of downwash and to isolate thereby the damping due to constant pitching velocity:

$$C_{m_q} = \frac{C_{m_q(\text{total})} - C_{m_q(\text{tail off})}}{1 + \frac{d\epsilon}{d\alpha}} + C_{m_q(\text{tail off})} \qquad (1)$$

where values of C_{m_q} in right-hand side of equation are measured values. Equation (1) is based on the assumption that the lag of downwash at the tail is proportional to the geometric tail length. Reference 9, however, indicates that in cases of unsteady lift the effective tail

length is in general greater than the geometric tail length so that equation (1) becomes

$$C_{m_q} = \frac{C_{m_{q(\text{total})}} - C_{m_{q(\text{tail off})}}}{1 + \frac{d\epsilon}{d\alpha}\frac{l_e}{l}} + C_{m_{q(\text{tail off})}} \qquad (1a)$$

The variation of angle of downwash with angle of attack $d\epsilon/d\alpha$ can be determined from wind-tunnel force tests. The results in reference 9 show that the effective tail length is equal to approximately 1.3 times the geometric tail length for a typical case. This ratio was used to correct values of $C_{m_{q(\text{tail on})}}$ for the present paper because the models with tail on (models 2 and 6) closely simulated the typical case. The effective tail length for any other case can be calculated from reference 9.

Investigations of models 1 and 3 revealed such small sidewash that the correction for lag of sidewash similar to that for the lag of downwash was negligible. Sufficient data were not available for the other models to determine sidewash; consequently, no attempts were made to include sidewash corrections in measurements of C_{n_r} for these models in the present paper.

Calculations

Damping in yaw.- Calculations of the rotary damping in yaw for an isolated wing were made by use of the empirical formula from reference 2

$$C_{n_r} = -0.33\left(\frac{1+3\lambda}{2+2\lambda}\right)C_{D_o} - 0.020\left(1 - \frac{A-6}{13} - \frac{1-\lambda}{2.5}\right)C_L{}^2 \qquad (2)$$

For flaps deflected, the following formula from references 2 and 6 was used:

$$C_{n_r} = -0.33\left(\frac{1+3\lambda}{2+2\lambda}\right)C_{D_o} - 0.33\left(\frac{b_f}{b}\right)^3\left[\frac{4-3\frac{b_f}{f}(1-\lambda)}{2+2\lambda}\right]\Delta C_{D_{of}}$$

$$+ K_1 C_{L_w}{}^2 + K_2\,\Delta C_{L_f}\,C_{L_w} + K_3\,\Delta C_{L_f}{}^2$$

where K_1, K_2, and K_3 are obtained from charts given in reference 6.

The increment of damping in yaw that is produced by the vertical tail located in the plane of symmetry was calculated from the following formula from reference 2:

$$\Delta C_{n_{r_t}} = -2\frac{l}{b}\Delta C_{n_{\beta_t}} \tag{4}$$

For vertical tails located on the wing the following formula was used to calculate the tail contribution to C_{n_r}:

$$\Delta C_{n_{r_t}} = -2\frac{l}{b}\Delta C_{n_{\beta_t}} - 4\left(\frac{y}{b}\right)^2 \Delta C_{D_t} \tag{5}$$

The derivation of equation (5) is given in the appendix. For tails at the wing tips $\frac{y}{b} = \frac{1}{2}$ and equation (5) becomes

$$\Delta C_{n_{r_t}} = -2\frac{l}{b}\Delta C_{n_{\beta_t}} - \Delta C_{D_t} \tag{5a}$$

For correlation with values obtained from the damping tests, which were made at low Reynolds number, values of C_{D_o}, $\Delta C_{D_{o_f}}$, and ΔC_{D_t} used in the present calculations were obtained from force tests at comparable Reynolds numbers. Values of the static directional stability provided by the vertical tail $\Delta C_{n_{\beta_t}}$ used in the calculations were also obtained from free-flight-tunnel force tests.

Damping in pitch.- The damping in pitch of an isolated wing was calculated by use of references 5 and 10. Reference 5 gives the variation of damping in uniform pitching motion with geometric and aerodynamic characteristics and position of the axis of rotation for an isolated wing; reference 10 gives the variation of damping with oscillation frequency. The following formula derived

from reference 5 gives the value of C_{m_q} for an isolated wing in uniform pitching motion:

$$C_{m_q} = C_{m_{q_{a.c.}}} - C_{L_{q_{a.c.}}}\left(\frac{x}{c}\right) - 114.6\frac{dC_L}{d\alpha}\left(\frac{x}{c}\right)^2 \qquad (6)$$

Values of $C_{m_{q_{a.c.}}}$ and $C_{L_{q_{a.c.}}}$ were obtained from tables of reference 5 where in they correspond to $-4q_o$ and $4z_o$, respectively. In order to obtain damping at a given frequency, equation (6) was corrected for oscillation effects by the data of figure 5 of reference 10. This correction was applied by multiplying the equation by the ratio of the oscillation damping parameter at the given frequency to the circular-motion damping parameter.

The damping in pitch produced by the horizontal tail $\Delta C_{m_{q_t}}$ was calculated from the formula

$$\Delta C_{m_{q_t}} = 2\frac{l}{c}C_{m_{i_t}} \qquad (7)$$

For all calculations the static derivative $C_{m_{i_t}}$ was obtained from force-test data.

RESULTS AND DISCUSSION

A complete summary of the experimental results of the damping tests for each model is presented in figures 1 to 12. The various configurations tested and the extent of the investigation for each model are given in table I.

Interpretation of Data

Damping in yaw.- Because of the difference in Reynolds number between model tests and full-scale flight, values of profile drag for models are larger than those for full-scale airplanes. The contribution of the profile drag to the total damping in yaw, however, is small and complete model tests are believed to give good qualitative

indications of C_{n_r} for full-scale airplanes. The incremental values of C_{n_r} for the wing and flaps, will be appreciably larger than full-scale values because the part of model damping due to profile drag is increased by the low scale of the tests.

Damping in pitch.- Although the value of C_{m_q} is dependent upon the value of the lift-curve slope, values of C_{m_q} obtained in the free-flight-tunnel tests are believed to be directly applicable to full-scale configuations. This conclusion is based on the fact that the tail lift-curve slopes for the two conventional models tested (models 2 and 6) were found to be approximately equal to the tail lift-curve slopes obtained on similar models at higher Reynolds numbers. Changes in C_{m_q} due to scale effect upon wing lift-curve slope will be unimportant because of the small magnitude of the wing damping.

Damping in Yaw

Contribution of wing to C_{n_r}.- The results of damping-in-yaw tests of several tailless models without vertical tails and of a wing alone are presented in figure 13. The data of figure 13(a) show the damping in yaw of a rectangular wing of aspect ratio 6 to be lower than would be predicted from references 3 and 4. (The original values of C_{n_r} presented in reference 4 are in error and the errata sheet must be used for the correct values.) The solid curve of figure 13(a) represents formula (2), which is an empirical formula developed in reference 2 from these experimental data.

The results of damping-in-yaw tests of the tailless models (figs. 13(b) to 13(d)) show C_{n_r} to vary inconsistently but to have values of the same order of magnitude as calculations from formula (2) although this formula is for an isolated wing. Formula (2) should,

therefore, satisfactorily predict values of C_{n_r} for tailless airplanes with the exception, of course, of the vertical-tail contribution.

Contribution of flaps to C_{n_r}.- Figure 14 shows the effect of deflecting 60-percent-span flaps on C_{n_r} for an isolated wing. The test data and calculations made by use of equations (2) and (3) show flap deflection to give a small increase in C_{n_r} at low lift coefficients. At high lift coefficients the calculations indicate that flap contribution to C_{n_r} decreases with lift coefficient, which results in a negligible effect, and the data agree with the calculated values except at a lift coefficient of approximately 1.6. Inasmuch as the total variation in C_{n_r} with flap deflection (both experimental and calculated) is small, it is believed that normal use of partial-span flaps will not appreciably affect the damping in yaw.

Figure 15 shows the effect of deflecting full-span flaps 40° upon the damping-in-yaw characteristics of a conventional and a tailless model, both without vertical tails. These data show that the full-span flaps give an appreciable and approximately constant contribution to C_{n_r} over the entire lift range. Values calculated from equations (2) and (3) are in fairly good agreement with experimental results.

The effect upon C_{n_r} of deflecting an unusual flap arrangement on a tailless model (model 10) is shown in figure 16. This flap arrangement consisted of a 33-percent-span lift flap deflected downward 60° in conjunction with 20-percent-span wing-tip pitch flaps deflected upward 40° for trimming purposes. The data show that this arrangement increased C_{n_r} at low values of lift coefficient and reversed the variation of C_{n_r} with lift coefficient. The smallest values of C_{n_r} with flaps

down were obtained at the highest lift coefficients.

The decrease in damping with lift coefficient is believed to occur as follows: At low angles of attack the tip sections of the wing operate at negative lift coefficients when the pitch flaps are deflected upward. An increase in the wing angle of attack, therefore, increases the lift and induced drag of the inboard sections but reduces the negative lift and induced drag of the tip sections. Inasmuch as the moment arms of the tip sections are greater than those of the inboard sections, the effects of the tip sections predominate and produce a net decrease in C_{n_r} with increasing lift coefficient.

Contribution of fuselage to C_{n_r}.- The results of tests made to determine the contribution of the fuselage to damping in yaw are presented in figure 17. The tests of the two isolated fuselages illustrate the insignificance of fuselage damping. The wing alone and vertical-tail-off data for model 4 indicate negligible effect of fuselage interference upon wing damping.

Experimental values of damping in yaw of various wing-fuselage combinations compared with values calculated for the wing alone are given in figure 18. These data also indicate that normal-size fuselages have little effect on C_{n_r} because the calculated and test values do not differ appreciably. Other tests reported in reference 2 have also indicated that the effect of a normal-size fuselage is small, probably ranging from $C_{n_r} = -0.003$ to -0.006. In general, therefore, the contribution of the fuselage to C_{n_r} may be expected to be small and can be neglected except possibly in cases in which the fuselage is very large or has flat sides.

Contribution of vertical tail to C_{n_r}.- The results in figure 19 show calculated and experimental effects of varying the vertical-tail area and moment arm upon the tail contribution to damping in yaw. The data show that C_{n_r} due to the tail increases approximately linearly with tail area and as the square of the tail moment

arm as predicted by theory. Test results and calculations made by equation (4) indicate a slight reduction in vertical-tail effectiveness as larger tails are used (fig. 19), which may be due to an increasingly smaller effective endplate provided by the horizontal tail.

Figure 20 shows the damping in yaw and static directional stability contributed by several vertical tails on model 4. The data indicate that the contribution of the tail to C_{n_r} when flaps are undeflected varies approximately as the contribution of the tail to static directional stability $\Delta C_{n_{\beta t}}$ and verifies the validity of equation (4). When flaps are deflected, however, the data indicate that equation (4) will not satisfactorily predict C_{n_r} as measured in an oscillation test. Sufficient force-test data on model 4 were not available to draw definite conclusions but perhaps flap deflection introduced sidewash effects that might account for the discrepancy between values of $C_{n_{r_t}}$ measured with flaps down and values calculated from equation (4). Further investigation of these effects appears to be necessary.

The effect of toe-in angle (the angle between vertical-tail chord line and airplane center line) on damping in yaw contributed by wing-tip vertical tails of three tailless models is shown in figure 21. The data and calculations from equation (5a) for model 11 indicate that an increase in tail contribution to C_{n_r} and C_{n_β} is obtained by toeing the tip fins inward. Calculations for models 12 and 12A from equation (5a) gave somewhat lower values of damping than experimental results.

Usually the tail contribution to C_{n_r} is essentially constant over the lift range but the data for model 7 (fig. 7) show a large variation. Inasmuch as force tests indicated only a relatively small increase in vertical-tail effectiveness with increasing lift coefficient the effects of lag of sidewash at the tail with this unorthodox design appears to introduce significant changes in the damping in yaw.

The over-all correlation of test data with calculated values for the tail contribution to C_{n_r} from equations (4) and (5a) is summarized in figure 22. The experimental results for power-off, flaps-up configurations show reasonable agreement with calculated values over large ranges of lift coefficient, tail design, and airplane type. Since no lag-of-sidewash corrections have been applied to any of the experimental C_{n_r} data, the correlation between measured and calculated values obtained in the tests is an indication that this factor is generally negligible for the power-off, flaps-up condition. The limited amount of data available for power-on and flaps-deflected conditions does not show satisfactory agreement of calculated and measured tail contribution to C_{n_r}. Both of these conditions probably introduce sidewash effects upon the damping characteristics of the tail.

The relative magnitude of vertical-tail damping in yaw for conventional and tailless designs can be observed from figure 22. For tailless designs the vertical-tail contribution to damping is roughly of the same magnitude as the wing-alone contribution. (See figs. 9 to 12.) For conventional designs, however, a high percentage ranging from 70 to 90 percent of the total damping in yaw is due to the vertical tail. (See figs. 1 to 8.) Damping in yaw of tailless airplanes range from about one-third to one-tenth that of conventional designs.

Contribution of propellers and slipstream to C_{n_r}.- Very little data are available concerning the effect of power upon damping in yaw. For two tailless models, windmilling propellers increased the damping in yaw less than 10 percent of the wing-alone value. (See figs. 9 and 10.)

Power-on data for a single-engine and a twin-engine model are presented in figure 23. These data show an increase in damping with thrust coefficient. The increase in C_{n_r} with thrust coefficient is much greater with the vertical tail on than with the vertical tail off and the increase is not so great when the tail is located out of the slipstream (model 5). The increased damping caused by

power effects appears, therefore, to result from the increased airstream velocity over the tail, which gives greater tail effectiveness. Further investigation, however, is required to clarify all the effects of power upon the damping in yaw.

Damping in Pitch

Contribution of wing to C_{m_q}.- Values of C_{m_q} measured for three tailless models are shown in figure 24. These data indicate no consistent variation of C_{m_q} over the lift-coefficient range tested. Values of C_{m_q} calculated by the methods of references 5 and 10 as described in the section of the present paper entitled "Calculations" are also presented in figure 24. These calculated values are larger than the measured values for all three models. Experiments have shown, however, that variations of C_{m_q} of this magnitude have negligible effect on the flight characteristics.

Contribution of flaps to C_{m_q}.- The effect of flap deflection upon the damping in pitch of a wing alone can be seen from data for the all-wing bomber model in figure 10. These data show negligible effect of deflecting flaps upon C_{m_q}. Inasmuch as flap deflection does not generally affect the lift-curve slope upon which C_{m_q} is largely dependent, this result is to be expected.

Contribution of fuselage to C_{m_q}.- An indication of fuselage damping in pitch can be obtained from C_{n_r} tests since a symmetrical fuselage at zero angle of attack has identical damping in pitch and yaw. The nondimensional damping parameters C_{n_r} and C_{m_q} are based on the span b and the mean aerodynamic chord c, respectively, so that

$$\Delta C_{m_{q(\text{fuselage})}} = \left(\frac{b}{c}\right)^2 \Delta C_{n_{r(\text{fuselage})}}$$

On this basis, since most fuselages are approximately symmetrical, the results for C_{n_r} previously discussed for fuselages indicate only a very small contribution of the fuselage to the damping in pitch (less than -0.2).

Contribution of horizontal tail to C_{m_q}.- The damping in pitch contributed by the horizontal tail of two models can be seen in figures 2 and 6. These data show that the tail is by far the most important component of the airplane contributing to C_{m_q} and that tails of normal size may be expected to provide 70 to 90 percent of the total damping in pitch of an airplane.

In figure 25 measured values of horizontal-tail damping in pitch are compared with calculated values based on equation (7). This comparison shows a fair agreement between calculated and measured results.

Contribution of propellers and slipstream to C_{m_q}.- Results of the effect of windmilling propellers on C_{m_q} are very similar to the effect on C_{n_r}. Tests showed that windmilling propellers increased the damping in pitch of two models by less than 10 percent. (See figs. 9 and 10.)

The effect of power on C_{m_q} for a twin-boom pusher fighter airplane model is shown in figure 26. These data show that, as might be expected with a pusher design, power had negligible effect on the tail-off damping in pitch but substantially increased the tail contribution to C_{m_q}. For the tail-on condition increasing power caused a higher value of C_{m_q}, which is attributed to the greater tail effectiveness resulting from the increased slipstream velocity over the tail.

CONCLUSIONS

The results of damping tests of 13 airplane models made in the Langley free-flight tunnel, which are summarized herein, and a comparison of these results with calculated results indicated the following conclusions:

1. Measured and calculated values of damping in yaw and in pitch for complete models were in satisfactory agreement for power-off, flaps-neutral conditions. Further research on the effects of sidewash on the damping in yaw for power-on and/or flaps-down conditions is needed.

2. Wing-alone damping was small and deflection of 60-percent-span flaps had little effect upon the damping in yaw and pitch. Deflection of full-span flaps, however, increased the damping in yaw but did not affect the damping in pitch.

3. The contribution of the fuselage to damping in yaw and pitch was generally negligible.

4. The tail surfaces contributed 70 to 90 percent of the rotational damping of conventional airplane designs.

5. Power tended to increase the tail effectiveness and thereby to increase damping in yaw and pitch.

6. The rotational damping of tailless airplanes was about one-third to one-tenth as large as that of conventional designs.

Langley Memorial Aeronautical Laboratory
National Advisory Committee for Aeronautics
Langley Field, Va., March 27, 1946

APPENDIX

Damping in Yaw of Wing-Tip Vertical Tails

The damping in yaw of wing-tip vertical tails may be considered to consist of the following two components:

(1) C_{n_r} due to change in effective angle of sideslip on the tails caused by the yawing velocity. This damping is similar to that produced by conventional vertical tails and is given by equation (4)

$$\Delta C_{n_{r_t}} = -2\frac{l}{b}\Delta C_{n_{\beta_t}}$$

where l is the front-and-back tail length.

(2) C_{n_r} due to the difference in drag of the two tails resulting from velocity differences at the tails. By definition, the speed of the leading and trailing tails, respectively, can be expressed as

$$V_L = V + ry$$

and

$$V_T = V - ry$$

Similarly the drag of the leading and trailing tails, respectively, may be written

$$\frac{1}{2}\Delta C_{D_t}\frac{1}{2}\rho S V_L^2$$

and

$$\frac{1}{2}\Delta C_{D_t}\frac{1}{2}\rho S V_T^2$$

where ΔC_{D_t} is the total drag coefficient of both vertical tails based on the wing area. Then the yawing moment produced by the difference in drag on the two tails can be expressed as

$$\Delta N_t = -\left(\frac{1}{2}\Delta C_{D_t}\frac{1}{2}\rho S V_L^2 - \frac{1}{2}\Delta C_{D_t}\frac{1}{2}\rho S V_T^2\right)y$$

When $V + ry$ and $V - ry$ are substituted for V_L and V_T, and the expression is simplified

$$\Delta N_t = -\frac{1}{2}\Delta C_{D_t}\frac{1}{2}\rho S(4ryV)y = -\Delta C_{D_t}\rho S r V y^2$$

Reduction to coefficient form gives

$$\Delta C_{n_t} = \frac{\Delta N_t}{\frac{1}{2}\rho V^2 S b} = -2\,\Delta C_{D_t}\left(\frac{ry^2}{Vb}\right)$$

$$= -4\frac{rb}{2V}\,\Delta C_{D_t}\left(\frac{y}{b}\right)^2$$

and differentiation with respect to $\frac{rb}{2V}$ yields

$$\frac{\partial \Delta C_{n_t}}{\partial(rb/2V)} = \Delta C_{n_{r_t}}$$

$$= -4\left(\frac{y}{b}\right)^2 \Delta C_{D_t}$$

Then the total tail damping produced by the change in effective angle of sideslip and by the drag difference on the tails may be expressed as

$$\Delta C_{n_{r_t}} = -2\frac{l}{b}\,\Delta C_{n_{\beta_t}} - 4\left(\frac{y}{b}\right)^2 \Delta C_{D_t}$$

REFERENCES

1. Bramwell, F. H., and Relf, E. F.: Experiments on Models of Complete Aeroplanes. Part IV. - Determination of the Pitching Moment Due to Pitching for a Model Biplane at Various Inclinations to the Wind. R. & M. No. 111, British A.C.A., 1914.

2. Campbell, John P., and Mathews, Ward O.: Experimental Determination of the Yawing Moment Due to Yawing Contributed by the Wing, Fuselage, and Vertical Tail of a Midwing Airplane Model. NACA ARR No. 3F28, 1943.

3. Glauert, H.: Calculation of the Rotary Derivatives Due to Yawing for a Monoplane Wing. R. & M. No. 866, British A.R.C., 1923.

4. Pearson, Henry A., and Jones, Robert T.: Theoretical Stability and Control Characteristics of Wings with Various Amounts of Taper and Twist. NACA Rep. No. 635, 1938.

5. Glauert, H., and Gates, S. B.: The Characteristics of a Tapered and Twisted Wing with Sweep-Back. R. & M. No. 1226, British A.R.C., 1929.

6. Harmon, Sidney M.: Determination of the Damping Moment in Yawing for Tapered Wings with Partial-Span Flaps. NACA ARR No. 3425, 1943.

7. Shortal, Joseph A., and Osterhout, Clayton J.: Preliminary Stability and Control Tests in the NACA Free-Flight Wind Tunnel and Correlation with Full-Scale Flight Tests. NACA TN No. 810, 1941.

8. Jones, B. Melvill: Dynamics of the Airplane. Symmetric or Pitching Moments. Vol. V of Aerodynamic Theory, div. N, ch. II, sec. D, W. F. Durand, ed., Julius Springer (Berlin), 1935. p.48.

9. Jones, Robert T., and Fehlner, Leo F.: Transient Effects of the Wing Wake on the Horizontal Tail. NACA TN No. 771, 1940.

10. Glauert, H.: The Force and Moment on an Oscillating Aerofoil. R. & M. No. 1242, British A.R.C., 1929.

TABLE I

SCOPE OF DATA

Model	Type	Test	Test airspeed (ft/sec) approx.	Oscillation frequency (cycles per sec) approx.	C_L	Flaps	Power condition	$\frac{z_w}{s}$	$\frac{z_T}{s}$	$\frac{l}{s}$
Wing with NACA 10$\frac{3}{4}$ section	Wing alone	C_{n_r}	40 to 60	0.9	0 to 1.6	60 percent span	----------	------	------	----
1	Conventional low-wing fighter	C_{n_r}	35	0.9	0.1 to 0.8	----------	Propeller windmilling $T_c = 0$ $T_c = 0.26$ $T_c = 0.52$	0.178	Tail off 0.103	0.46
2	Twin-boom pusher fighter	C_{m_q}	30 to 40	2.0	0.4 to 2.1	Full span	$T_c = 0$ $T_c = 0.6$ $T_c = 1.2$	Tail off .206	.085	.53
3	Conventional parasol	C_{n_r}	40	0.9	0.2 to 1.2	----------	Propeller off	.154	Tail off .085	.44
4	Conventional midwing	C_{n_r}	30 45	0.6 1.1	0 to 1.9	Full span	Propeller off	.250	Tail off .050 .100 .150 .250	.50
5	Twin-engine mid-wing bomber	C_{n_r}	35	0.9	0.7	----------	$T_c = 0$ $T_c = 0.26$ $T_c = 0.52$	.271	.111	.39
6	Conventional mid-wing	C_{n_r}	40 to 60	1.6	0.2 to 1.0	----------	Propeller off	Tail off .080 .160 .240	Tail off .052 .105	.35
		C_{m_q}	30	1.0	0.1 to 0.6					
7	Glide bomb	C_{n_r}	60	1.3	0.1 to 0.9	----------	Propeller off	.179	Tail off .355	.62
8	Research Model	C_{n_r}	45	0.8	0.5 1.0	----------	Propeller off	.204	Tail off .025 .050 .075 .100	.20 .32 .50
9	Tailless pusher high-wing fighter	C_{n_r}	35	0.8	0.1 to 1.0	----------	Propeller off Propeller windmilling		Tail off .060	.24
		C_{m_q}	35	1.8	0.1 to 1.0					
10	Tailless pusher all-wing bomber	C_{n_r}	35	1.0	0.3 to 1.4	Center-section lift flap and wing-tip pitch flaps	Propeller off Propeller windmilling	------	Tail off .040	.10
		C_{m_q}	30 to 40	3.5	0.3 to 1.4					
11	Tailless all-wing cargo	C_{n_r}	40	1.5	0 to 0.7	----------	Propellers off	------	Tail off .100 (fuselage fin) .100 (tip fins)	.11 (fuselage fin) .024 (tip fins)
12	Tailless high-wing bomber	C_{n_r}	35	1.2	0 to 1.4	Full span	Propellers off	------	Tail off .075 (fuselage fin) .100 (tip fins)	.17 (fuselage fin) .085 (tip fins)
		C_{m_q}	35	3.2	.5 to 0.7					
12A	Tailless midwing bomber	C_{n_r}	45	1.7	0 to 1.3	85 percent span	Propellers off	------	.120 (tip fins)	.088 (tip fins)
		C_{m_q}	35 to 45	4.0	0.5 to 0.7					

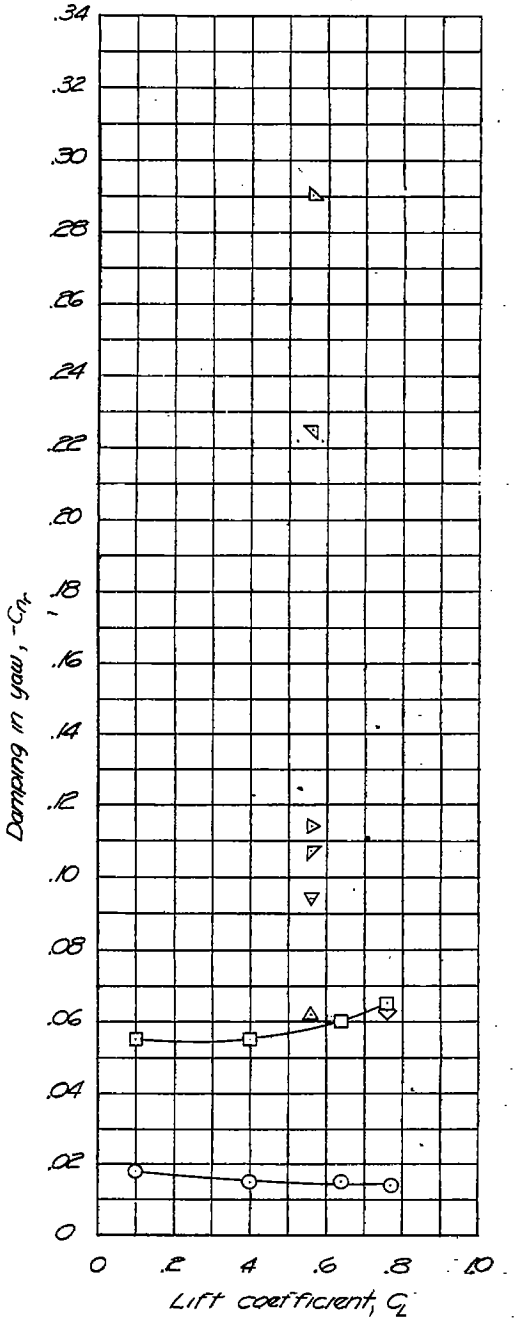

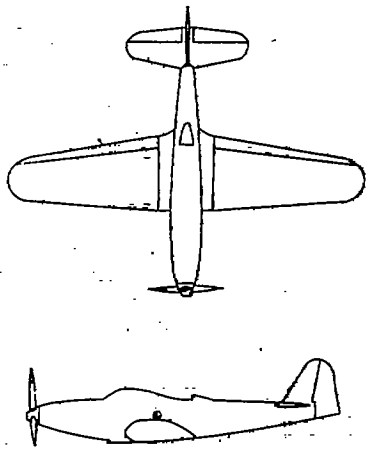

MODEL 1

Conventional low-wing fighter

Over-all length, ft	3.44
Dihedral, deg	5.5
Sweepback of .25 chord, deg	1
Wing area, sq ft	2.48
Wing span, ft	3.63
Aspect ratio	5.32
Taper ratio	.50
Mean aerodynamic chord, ft	.69
Tail length, ft	1.76
Vertical tail area, percent wing area	10.3
Horizontal tail area, percent wing area	17.2

	Vertical tail	Power condition
○	Off	Propeller windmilling
△	Off	$T_c = 0$
▽	Off	$T_c = 0.26$
▷	Off	$T_c = 0.52$
□	On	Propeller windmilling
◇	On	Propeller off
▽	On	$T_c = 0$
▽	On	$T_c = 0.26$
△	On	$T_c = 0.52$

NATIONAL ADVISORY
COMMITTEE FOR AERONAUTICS

Figure 1.- Damping in yaw for model 1.

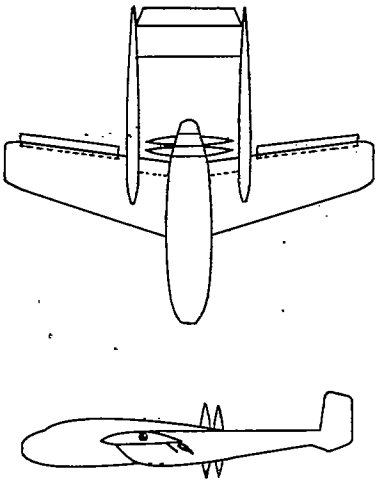

MODEL 2

Twin-boom pusher fighter

Over-all length, ft	3.67
Dihedral, deg	
Inboard	0
Outboard	5
Sweepback of .25 chord, deg	16
Wing area, sq ft	2.86
Wing span, ft	4.00
Aspect ratio	5.60
Taper ratio	.51
Mean aerodynamic chord, ft	.72
Tail length, ft	2.10
Flap chord, percent wing chord	
Inboard	18
Outboard	13
Vertical-tail area, percent wing area	12.2
Horizontal-tail area, percent wing area	20.6

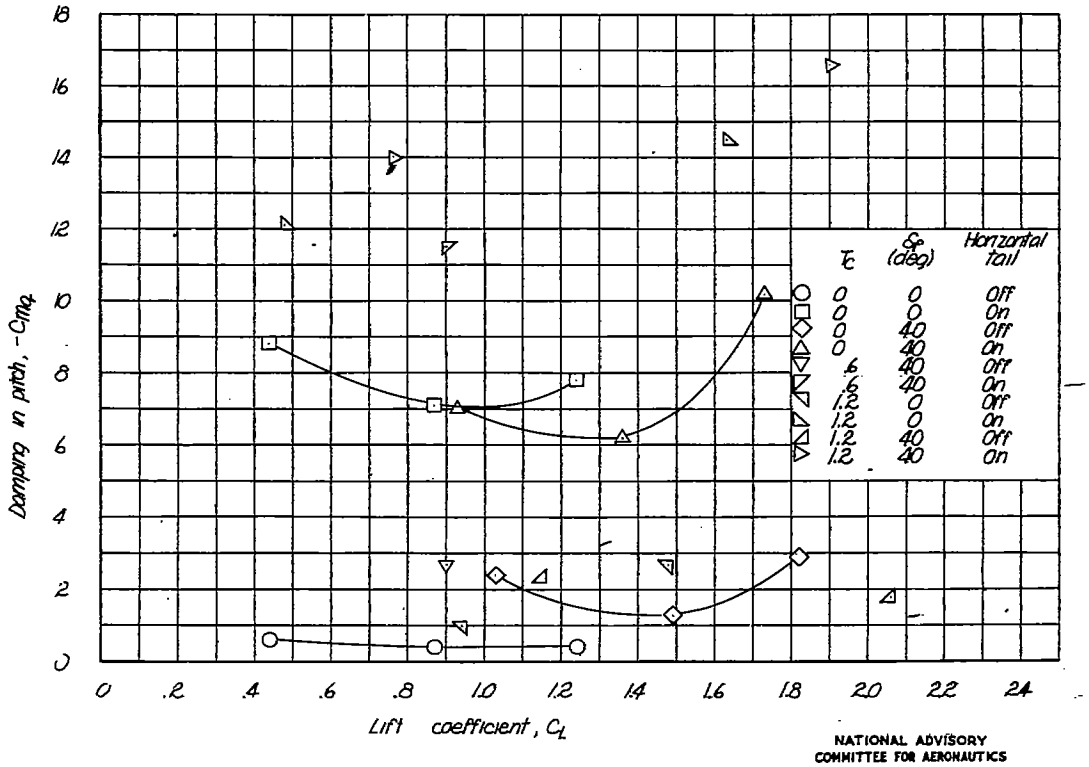

Figure 2.- Damping in pitch for model 2.

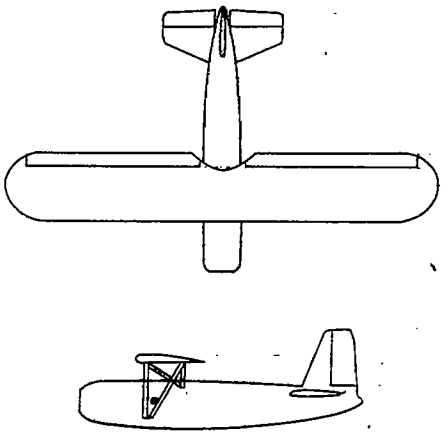

MODEL 3

Conventional parasol airplane

Over-all length, ft	3.14
Dihedral, deg	0
Sweepback of .25 chord, deg	0
Wing area, sq ft	4.47
Wing span, ft	4.75
Aspect ratio	6.50
Taper ratio	1.0
Mean aerodynamic chord, ft	.78
Tail length, ft	2.06
Vertical tail area, percent wing area	8.5
Horizontal tail area, percent wing area	15.4

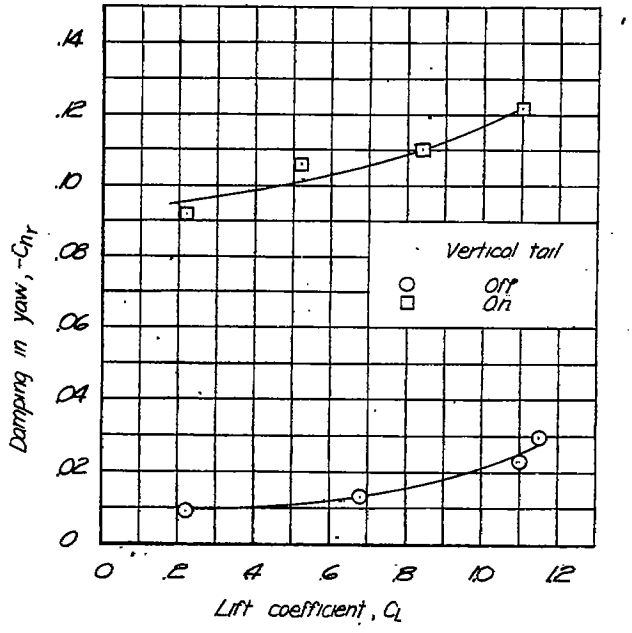

NATIONAL ADVISORY
COMMITTEE FOR AERONAUTICS

Figure 3.- Damping in yaw for model 3.

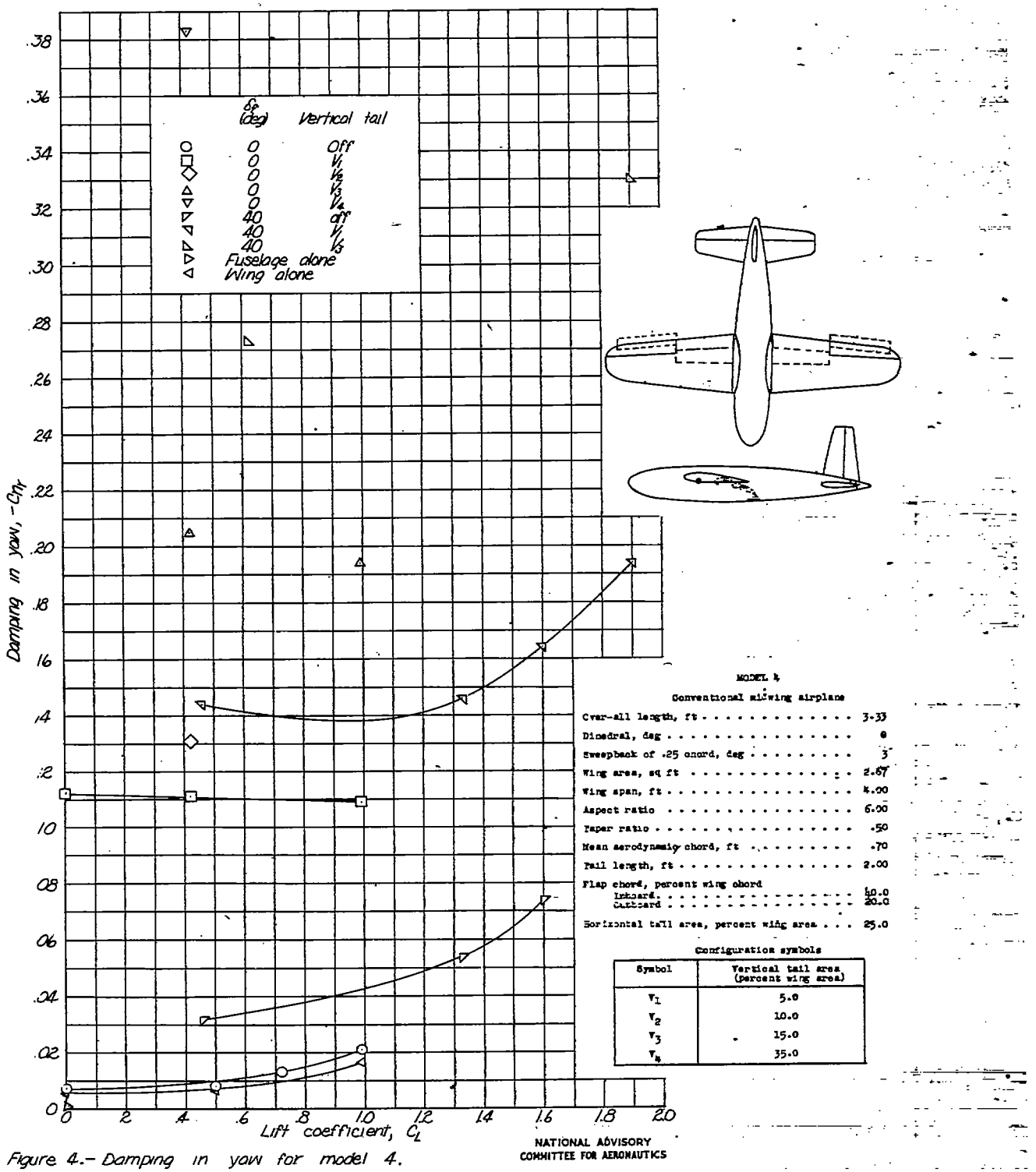

Figure 4.- Damping in yaw for model 4.

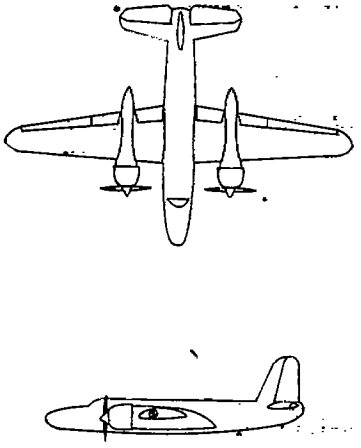

MODEL 5

Twin-engine midwing bomber

Over-all length, ft	2.72
Dihedral, deg	2
Sweepback of .25 chord, deg	2
Wing area, sq ft	1.09
Wing span, ft	3.54
Aspect ratio	7.80
Taper ratio	.42
Mean aerodynamic chord, ft	.50
Tail length, ft	2.34
Vertical tail area, percent wing area	11.1
Horizontal tail area, percent wing area	27.1

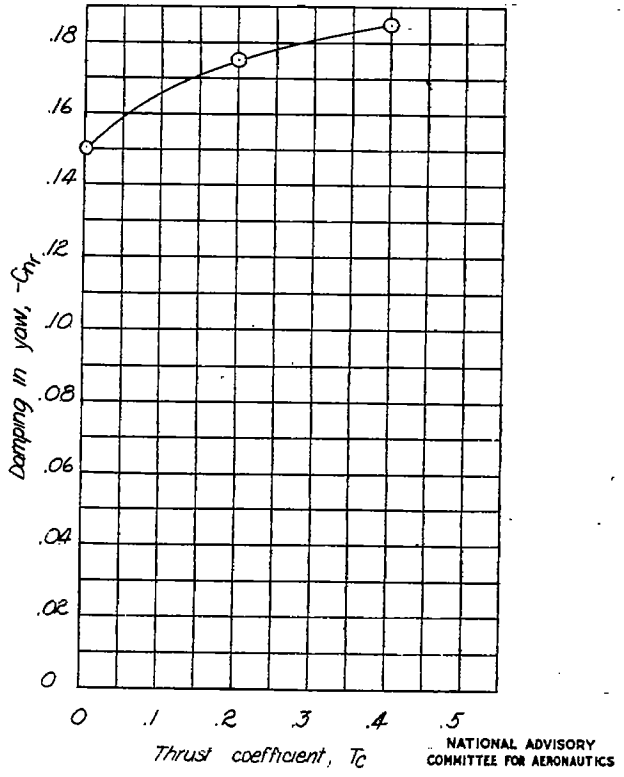

Figure 5.- Damping in yaw for model 5. $C_L = 0.7$

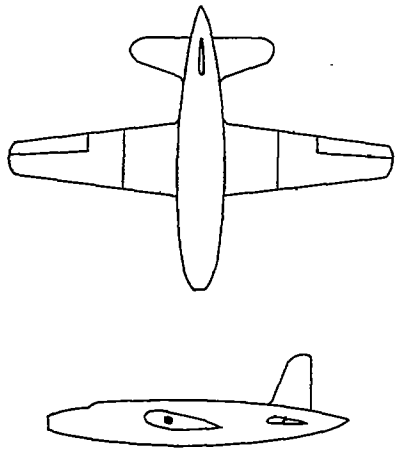

MODEL 6

Conventional midwing airplane

Over-all length, ft	2.99
Dihedral, deg	0
Sweepback of .25 chord, deg	2
Wing area, sq ft	2.26
Wing span, ft	3.90
Aspect ratio	6.73
Taper ratio	.40
Mean aerodynamic chord, ft	.62
Tail length, ft	1.37

Configuration symbols

Symbol	Configuration	Tail area (percent wing area)
S_{V_1}	Vertical tail	5.2
S_{V_2}	Vertical tail	10.5
S_{H_1}	Horizontal tail	8.0
S_{H_2}	Horizontal tail	16.0
S_{H_3}	Horizontal tail	24.0

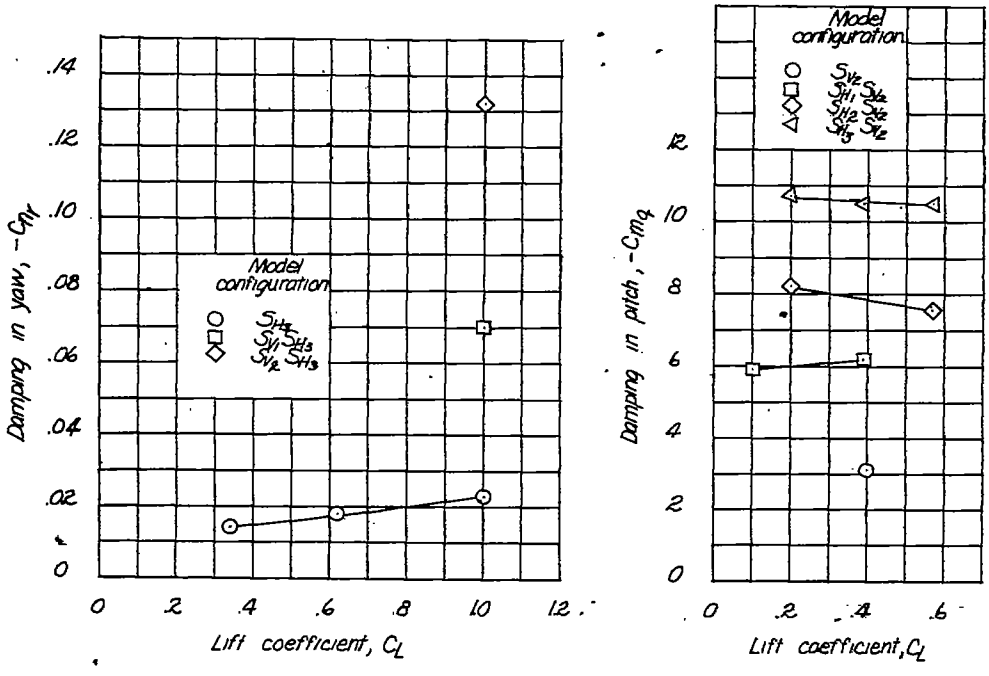

NATIONAL ADVISORY COMMITTEE FOR AERONAUTICS

Figure 6.- Damping in yaw and pitch for model 6.

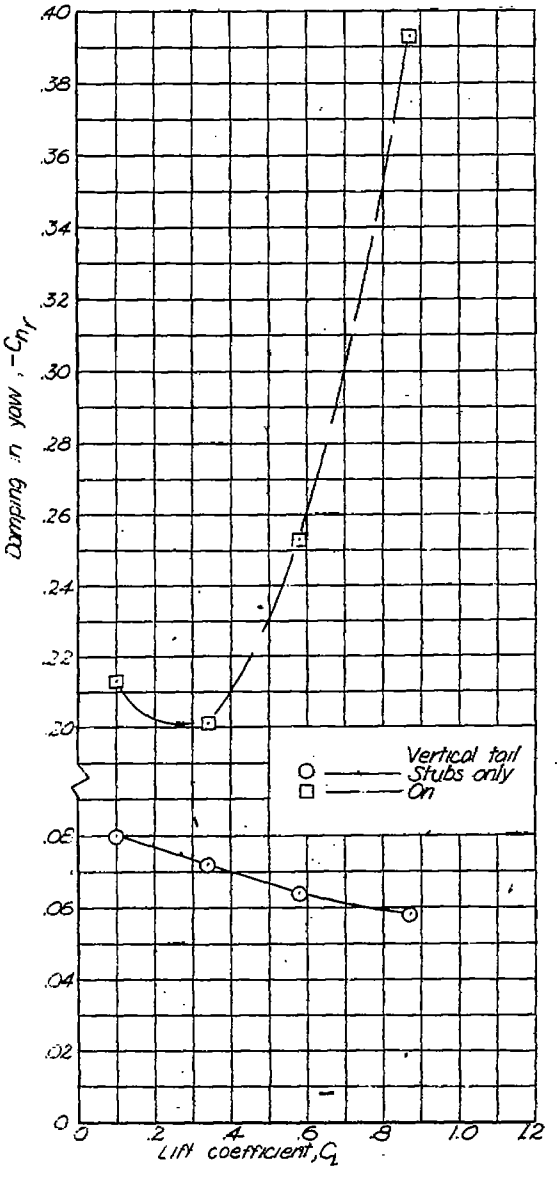

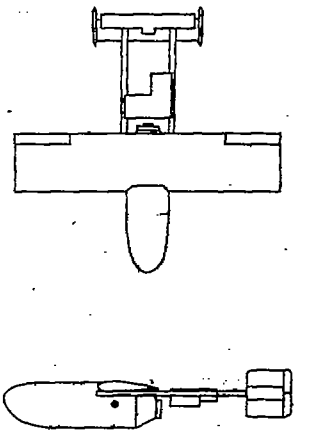

MODEL 7

Glide bomb

Over-all length, ft	3.80
Dihedral, deg	0
Sweepback of .25 chord, deg	0
Wing area, sq ft	2.08
Wing span, ft	3.00
Aspect ratio	4.33
Taper ratio	1.00
Mean aerodynamic chord, ft	.69
Tail length, ft	1.86
Vertical tail area, percent wing area	33.5
Total stub area, percent wing area	5.7
Horizontal tail area, percent wing area	17.9

NATIONAL ADVISORY
COMMITTEE FOR AERONAUTICS

Figure 7.- Damping in yaw for model 7.

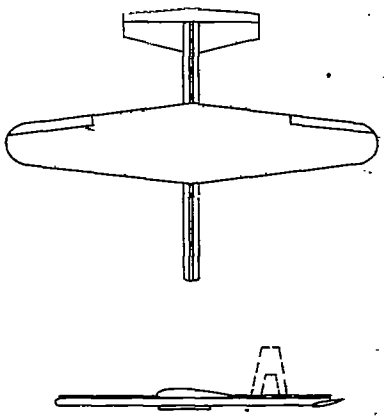

MODEL 8

Research model

Over-all length, ft	3.92
Dihedral, deg	0
Sweepback of .25 chord, deg	3
Wing area, sq ft	2.67
Wing span, ft	4.00
Aspect ratio	6.00
Taper ratio	.50
Mean aerodynamic chord, ft	.70
Tail lengths, ft	.80 1.40 2.00
Horizontal tail area, percent wing area	20.4

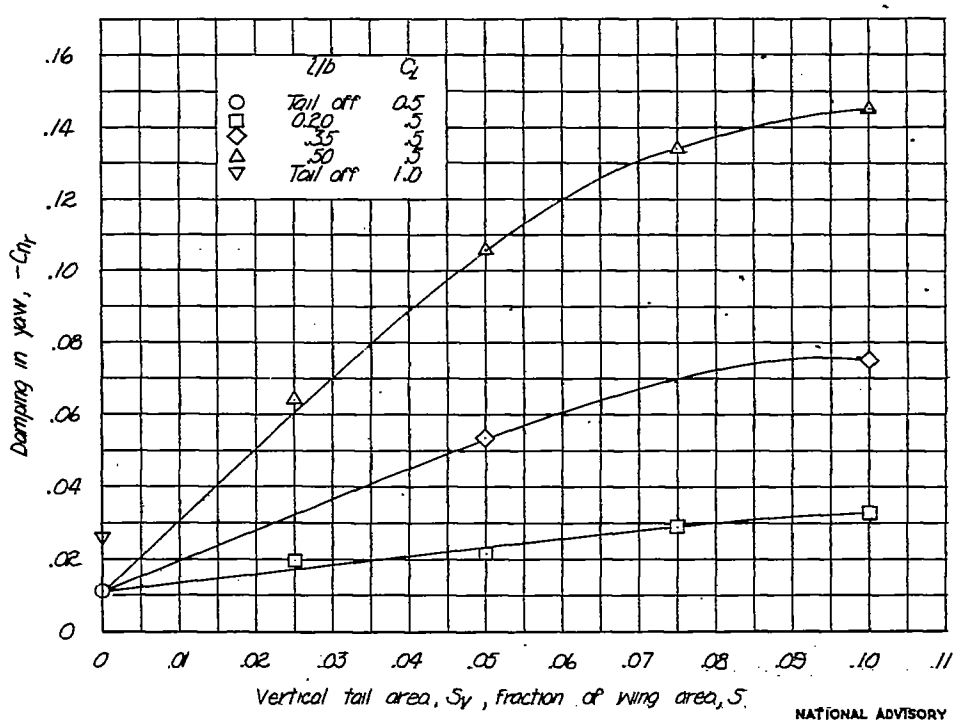

Figure 8.- Damping in yaw for model 8.

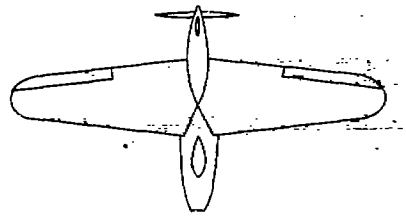

MODEL 9

Tailless pusher high-wing fighter

Over-all length, ft	2.31
Dihedral, deg	0
Sweepback of .25 chord, deg	3
Wing area, sq ft	2.67
Wing span, ft	4.00
Aspect ratio	6.00
Taper ratio	.50
Mean aerodynamic chord	.70
Tail length, ft	.96
Total vertical tail area, percent wing area	6.0

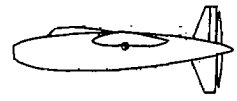

Configuration symbols

Symbol	Configuration
F	Fuselage
W	Wing
P	Windmilling propeller
V^1	Lower vertical tail
V^2	Upper vertical tail

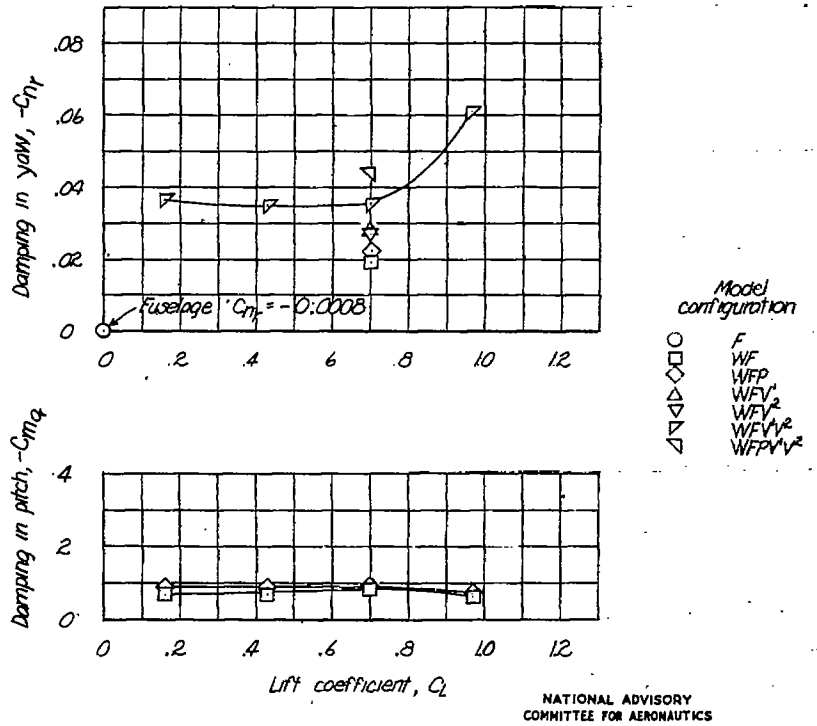

Figure 9.- Damping in yaw and pitch for model 9.

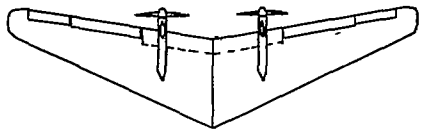

MODEL 10

Tailless pusher all-wing bomber

Over-all length, ft	1.28
Dihedral, deg	0
Sweepback of .25 chord, deg	22
Wing area, sq ft	2.52
Wing span, ft	4.30
Aspect ratio	7.34
Taper ratio	.25
Mean aerodynamic chord, ft	.86
Tail length, ft	.43
Flap chord, percent wing chord	25
Total vertical tail area, percent wing area	4.0

Configuration symbols

Symbol	Configuration
W	Wing and propeller shaft housings
P	Windmilling propellers
V	Vertical tails
F	Center section lift flaps down 60° and wing-tip pitch flaps up 40°

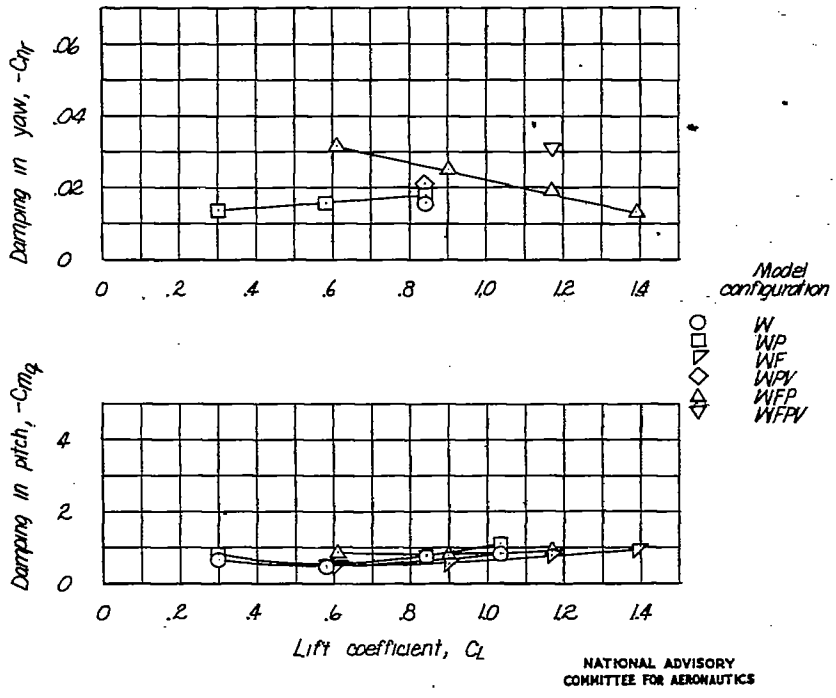

Figure 10.- Damping in yaw and pitch for model 10.

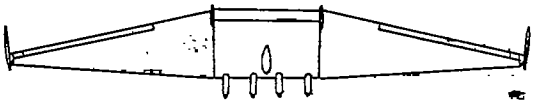

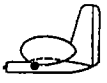

MODEL 11

Tailless all-wing cargo transport

Over-all length, ft	.60
Dihedral, deg	0
Sweepback of .25 chord, deg	0
Wing area, sq ft	2.20
Wing span, ft	4.84
Aspect ratio	10.60
Taper ratio	.20
Mean aerodynamic chord, ft	.62
Tail length, ft	
Fuselage fins	.53
Tip fins	.12

Configuration symbols

Symbol	Configuration	Tail area (percent wing area)
W	Wing and nacelles	—
V	Center section vertical tails	10.0
V_5	Wing-tip vertical tails toed in 5°	10.0
V_{10}	Wing-tip tails toed in 10°	10.0
V_{15}	Wing-tip tails toed in 15°	10.0

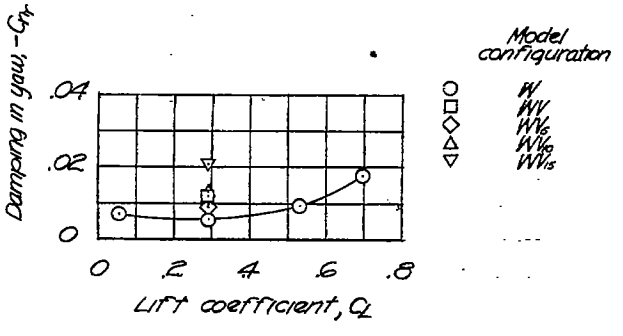

NATIONAL ADVISORY
COMMITTEE FOR AERONAUTICS

Figure 11.—Damping in yaw for model 11.

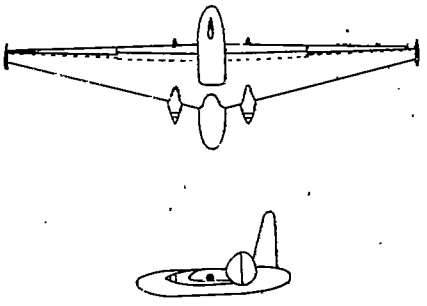

	MODEL 12 Tailless high-wing bomber (shown in sketch)	MODEL 12A Tailless midwing bomber (similar to model 12)
Over-all length, ft	1.65	1.40
Dihedral, deg	2	2
Sweepback of .25 chord, deg	2	11
Wing area, sq ft	2.00	1.47
Wing span, ft	4.47	4.20
Aspect ratio	10.00	12.00
Taper ratio	.17	.25
Mean aerodynamic chord, ft	.53	.39
Flap chord, percent wing chord Inboard Outboard	.25 .20	.28 ----
Flap span, percent wing span	1.00	.85
Tail length, ft Tip fins Fuselage fins	.37 .76	.37 ----
Vertical tail, percent wing area Tip fins Fuselage fins	10.0 7.5	12.0 ----

Configuration symbols

Symbol	Configuration
W	Wing and small fuselage
V_t	Wing-tip vertical tails toed in 5°
V_f	Fuselage vertical tail
F	Flaps down 40°

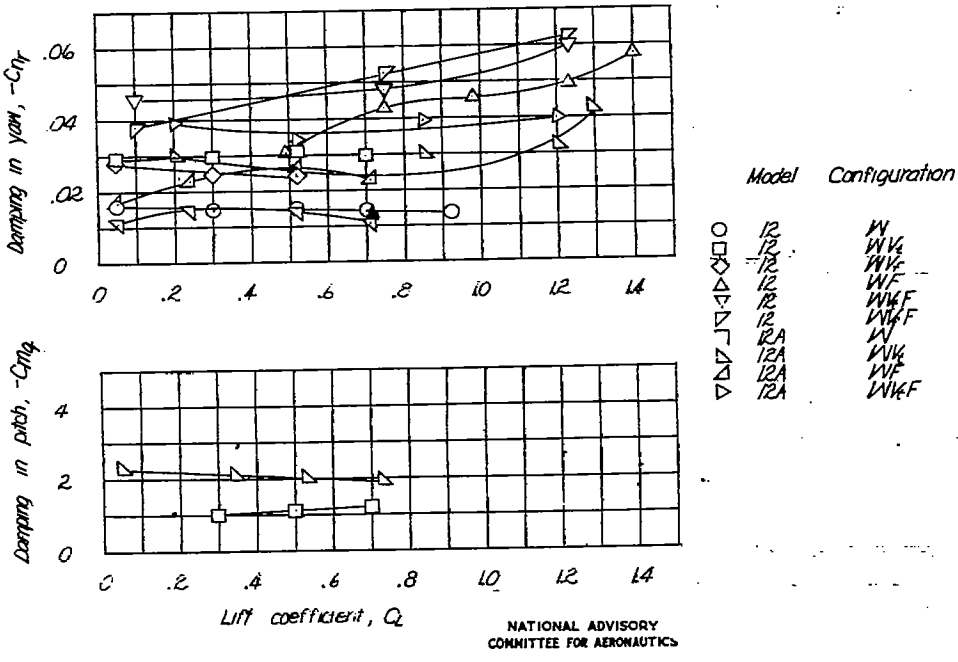

Figure 12.- Damping in yaw and pitch for models 12 and 12A.

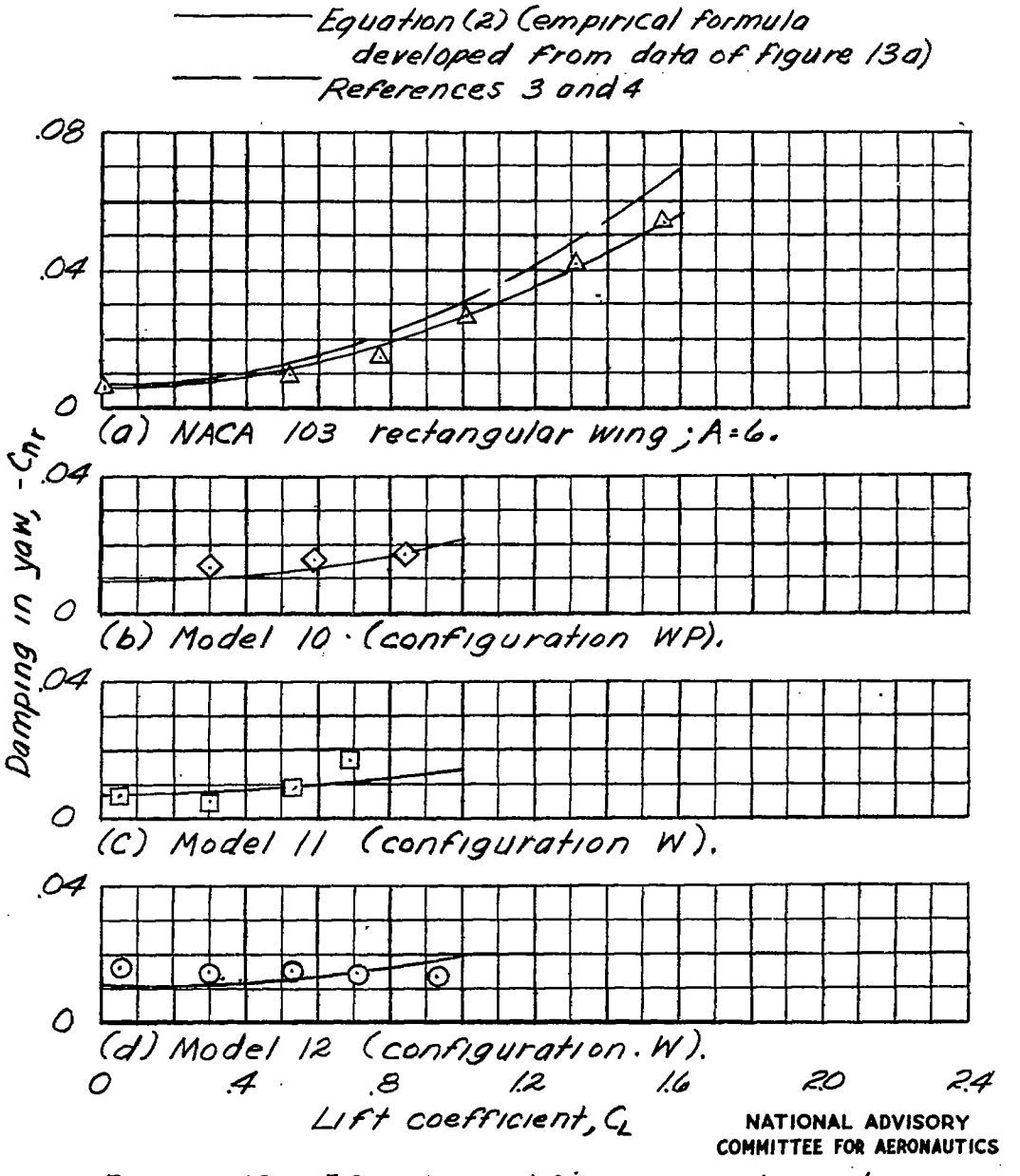

Figure 13. - Effect of lift coefficient on damping in yaw of wing alone and tailless models without vertical tails tested in Langley free-flight tunnel. All calculations are for wing alone.

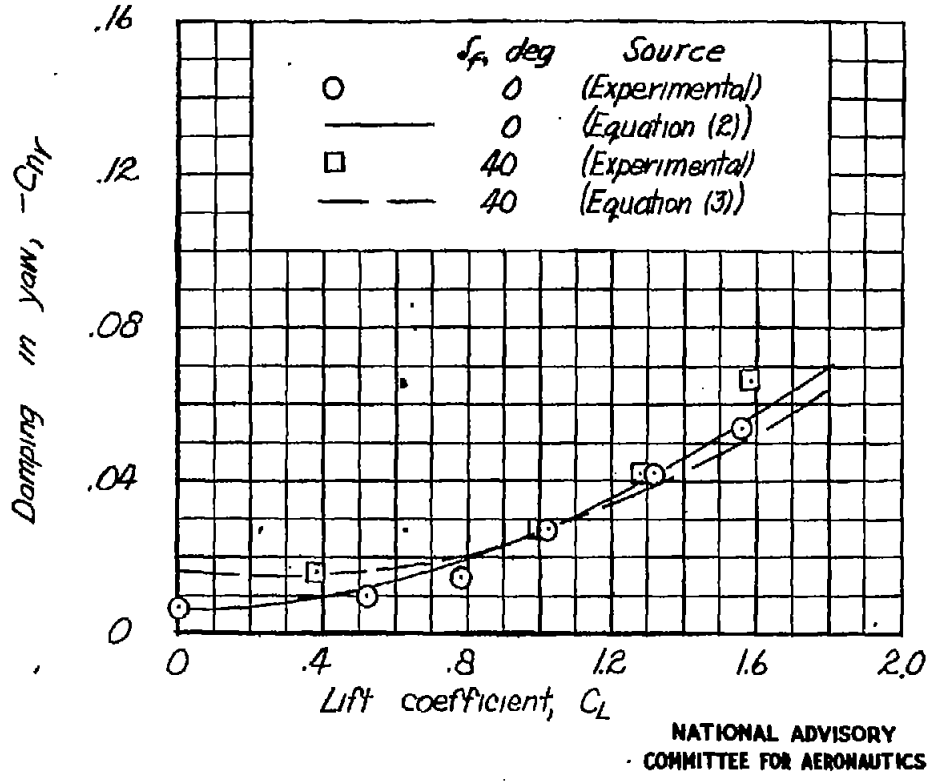

Figure 14.— Effect of deflecting 60-percent-span flaps on damping in yaw of an NACA 103 rectangular wing.

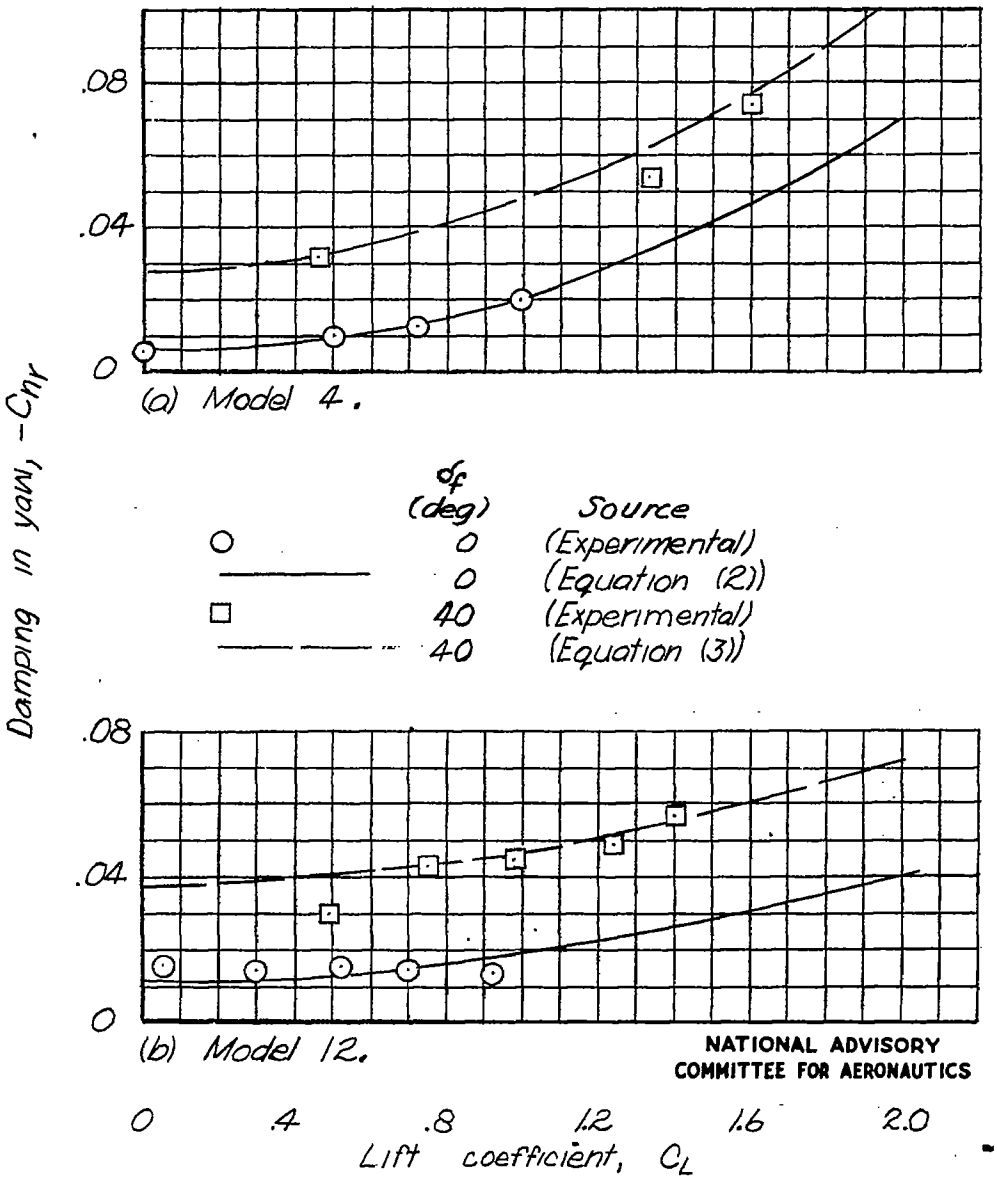

Figure 15. — Effect of deflecting full-span flaps on damping in yaw of conventional and tailless models with vertical tails off. All calculations are for wing alone and wing with flaps deflected.

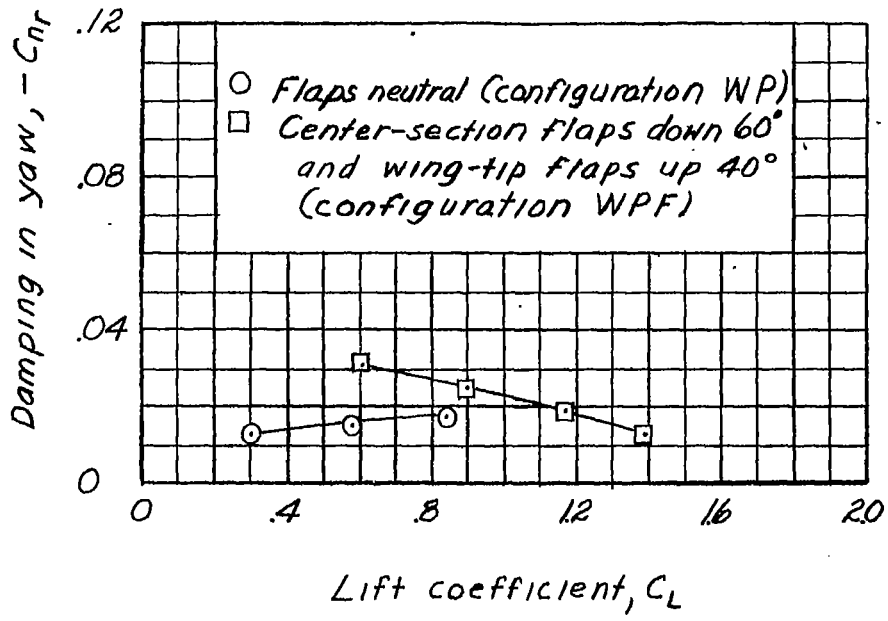

Figure 16.- Effect of deflecting center-section lift flaps and wing-tip pitch flaps on damping in yaw of model 10 without vertical tails.

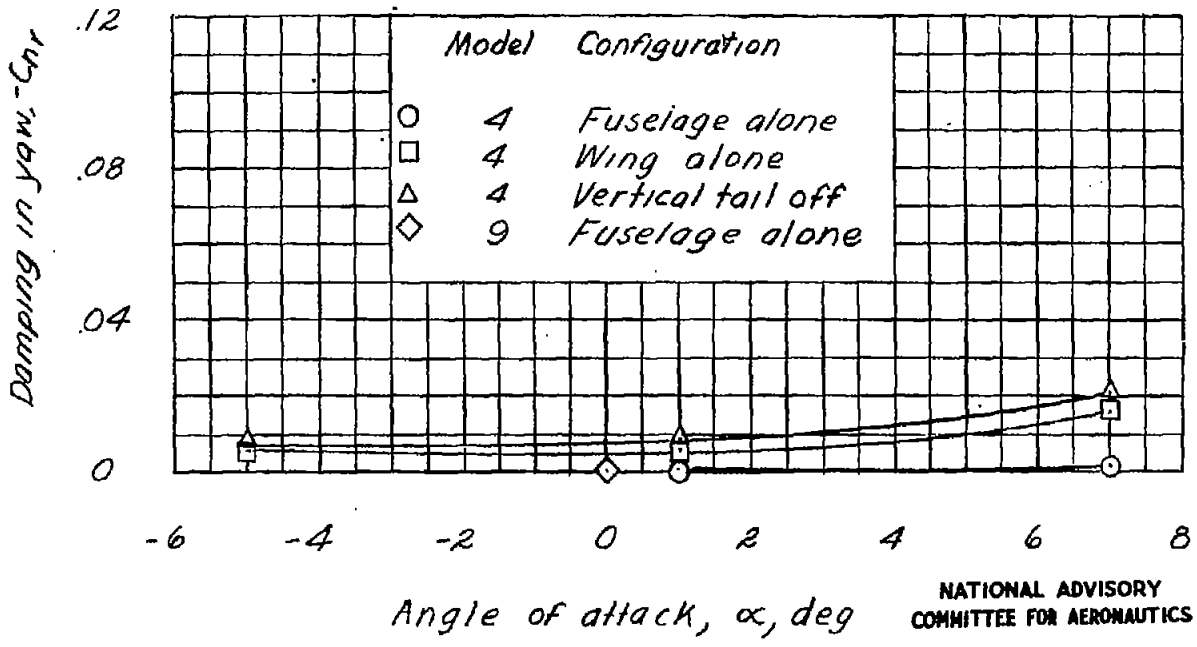

Figure 17.—Effect of fuselage on damping in yaw.

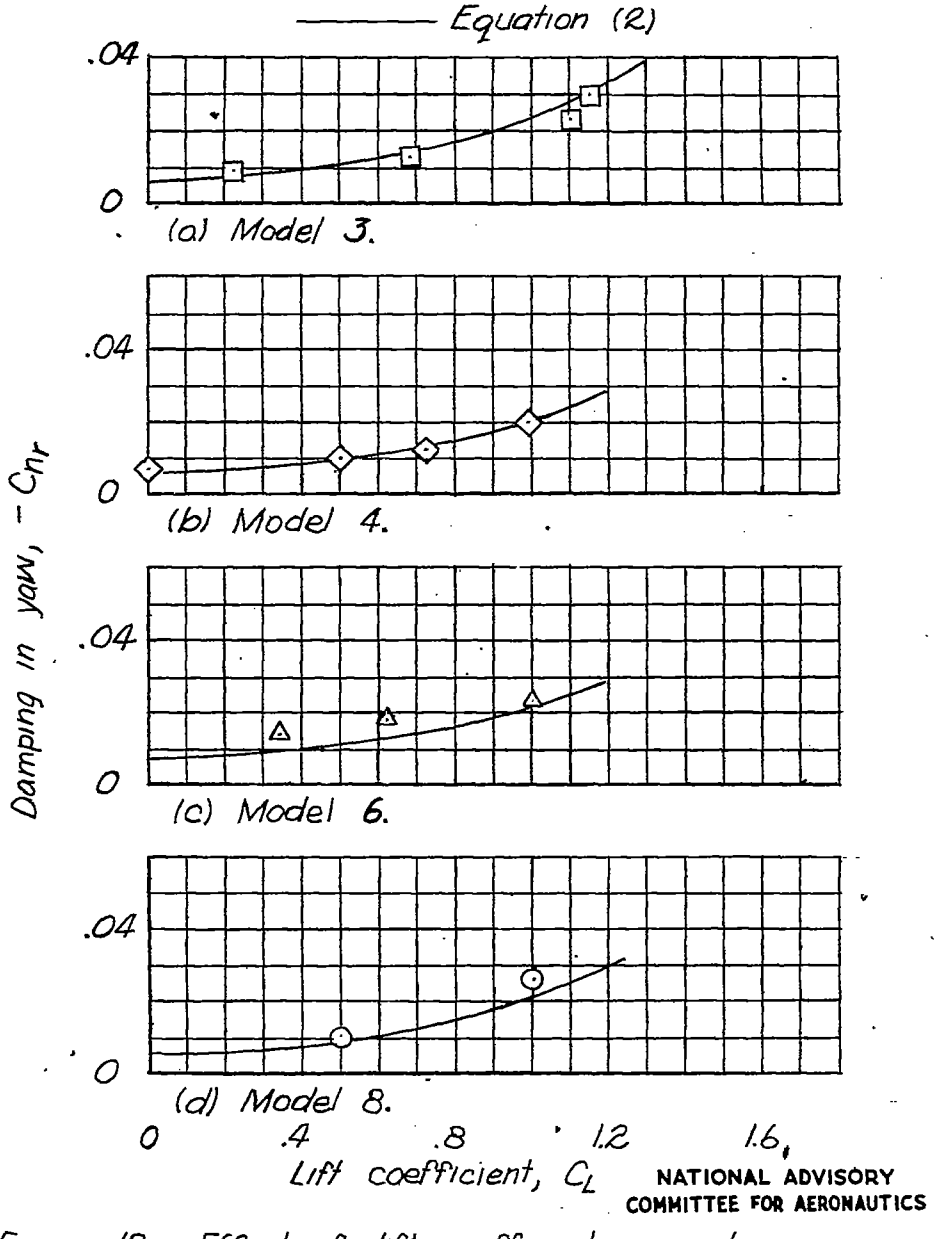

Figure 18.— Effect of lift coefficient on damping in yaw of conventional airplane models with vertical tails removed. All calculations are for wing alone.

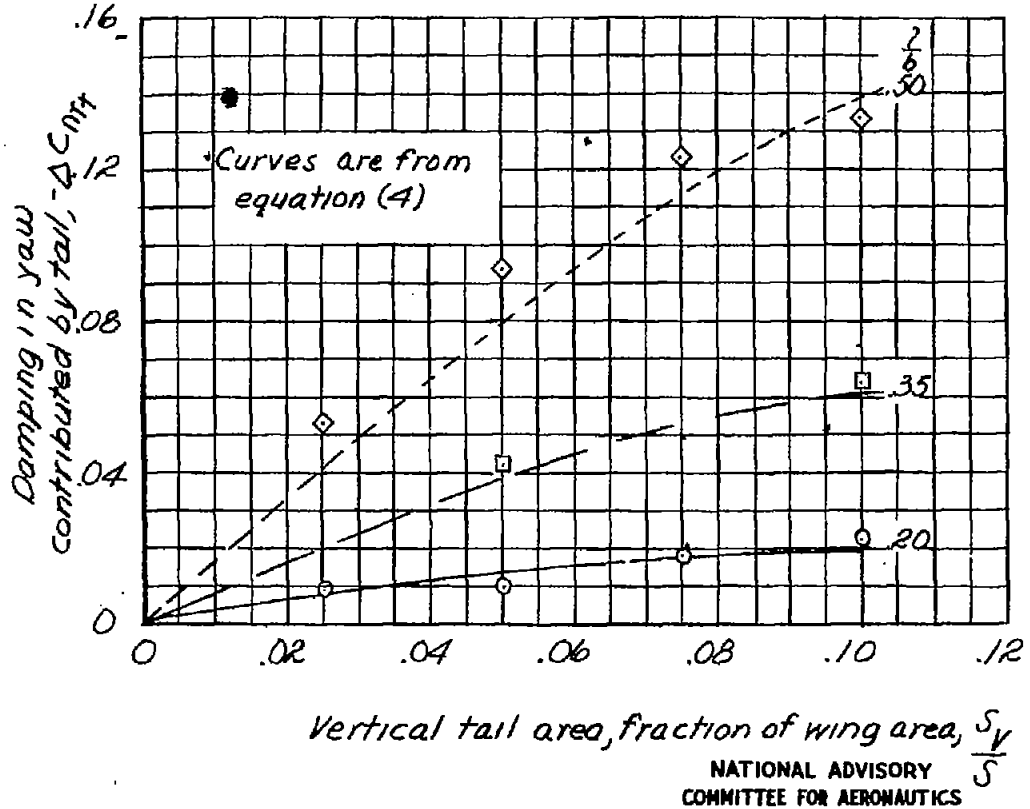

Figure 19.- Effect of tail area and length on damping in yaw contributed by tail. Model 8; $C_L = 0.5$.

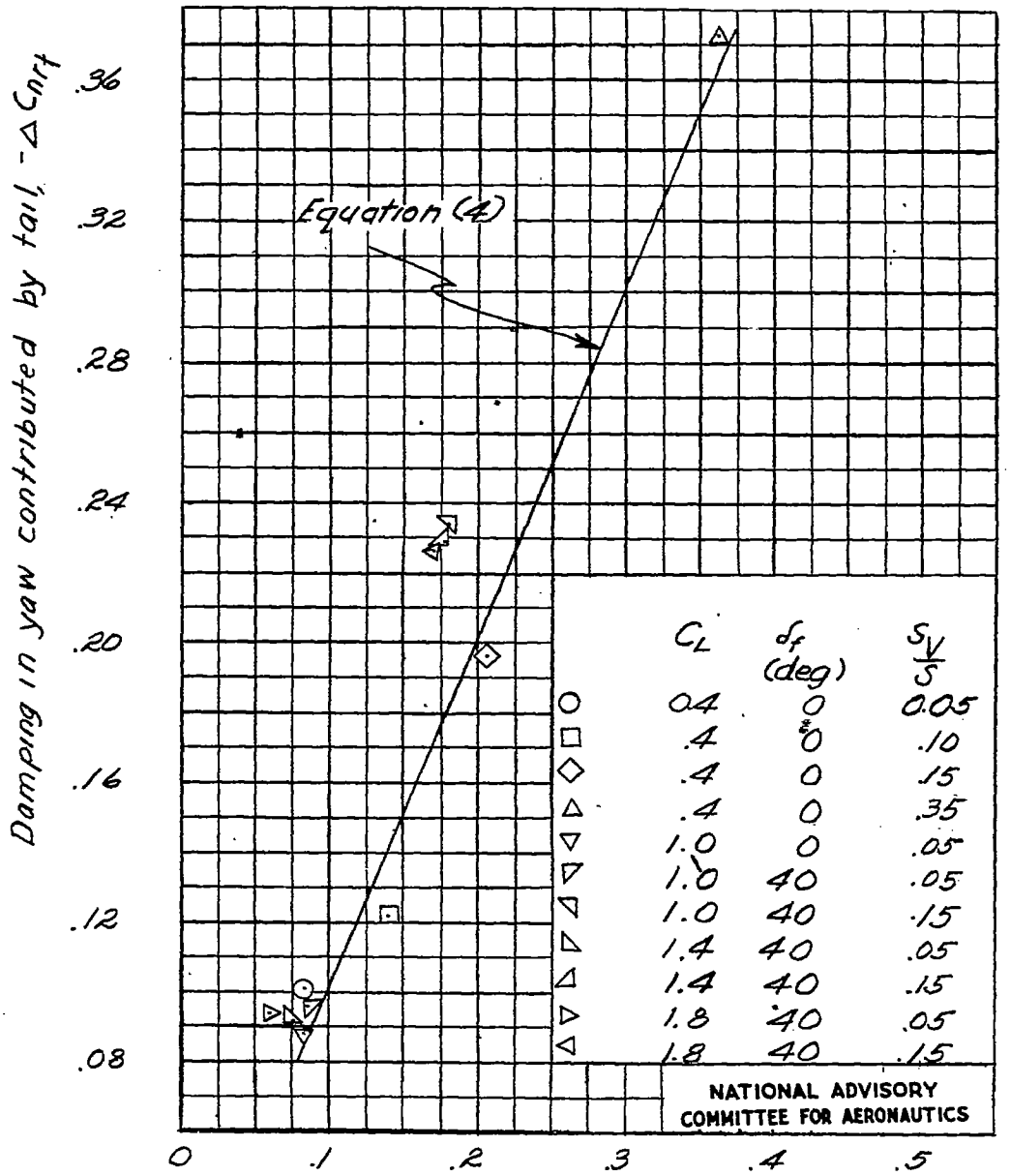

Figure 20. – Comparison of directional stability and damping in yaw contributed by the vertical tail for Model 4. $\frac{l_t}{b} = 0.50$.

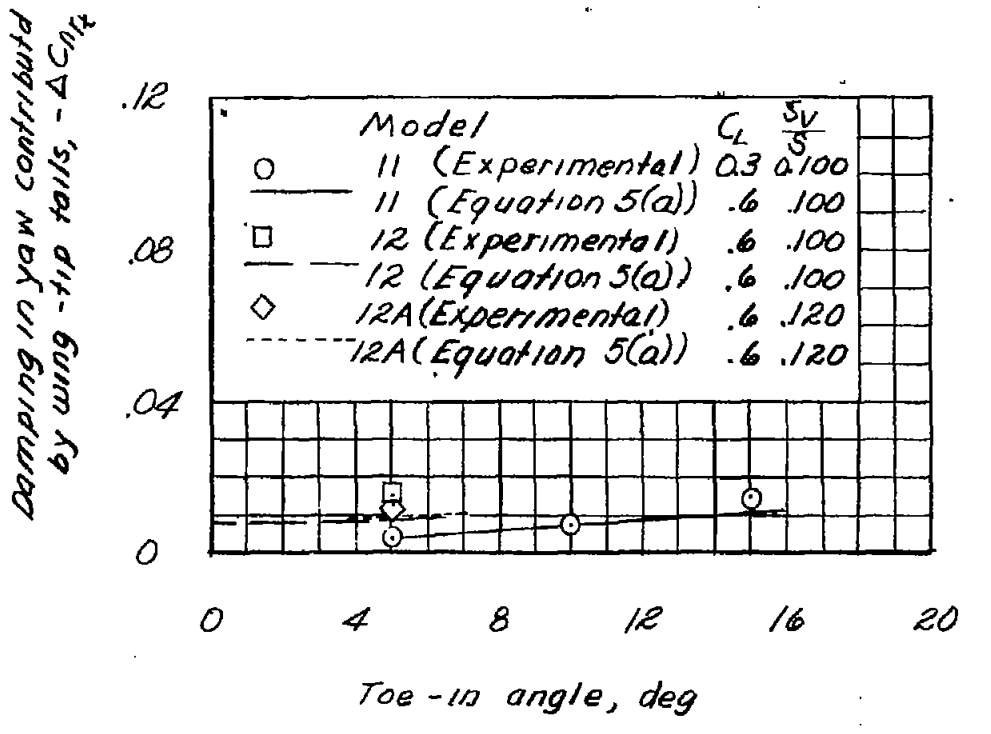

NATIONAL ADVISORY
COMMITTEE FOR AERONAUTICS

Figure 21. – Effect of toe-in angle on damping in yaw contributed by wing-tip vertical tails.

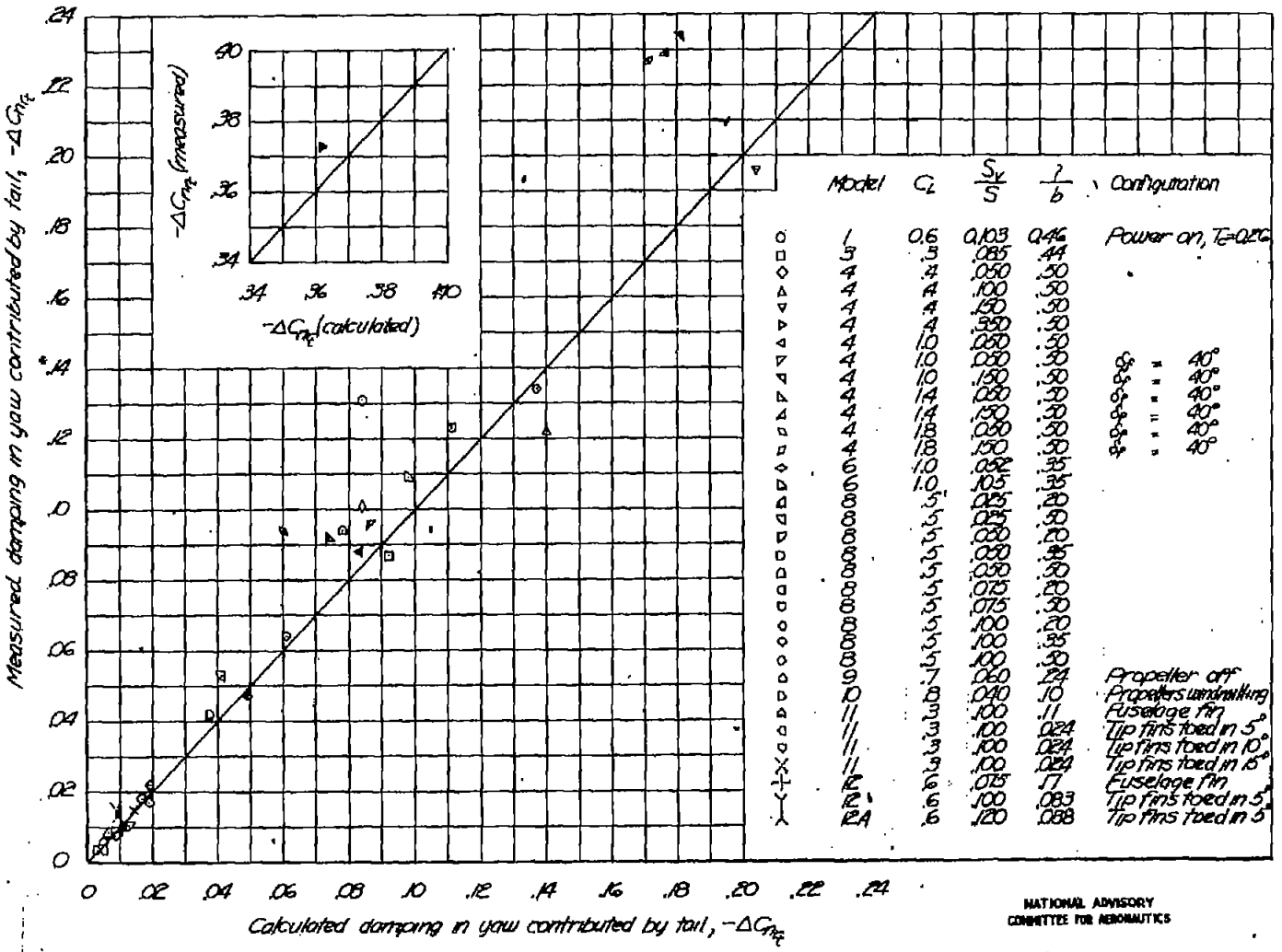

Figure 22.– Comparison of measured damping in yaw contributed by tail with calculated values from equation (4) and (5a) for a number of models tested in Langley free-flight tunnel.

Fig. 22

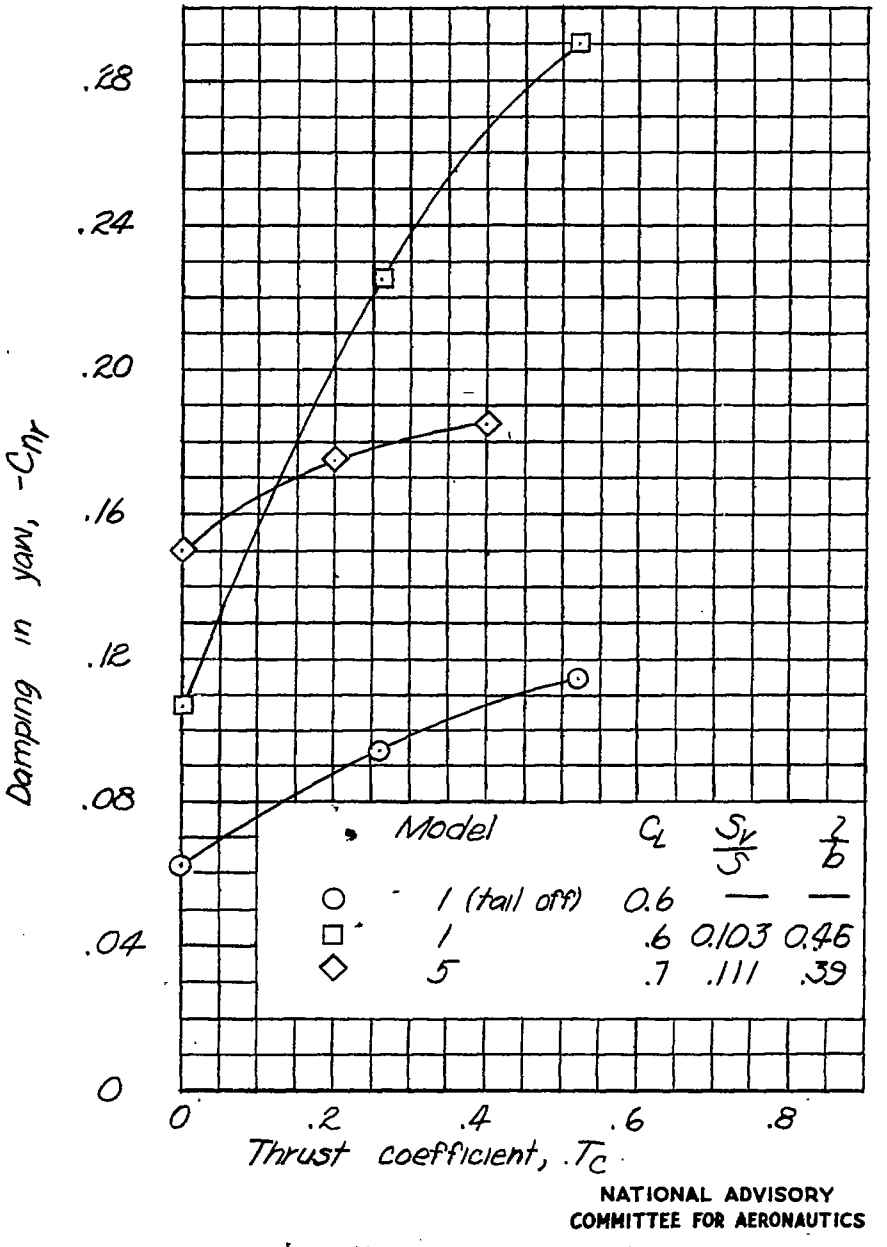

Figure 23. – Effect of thrust coefficient on damping in yaw of two conventional airplane models.

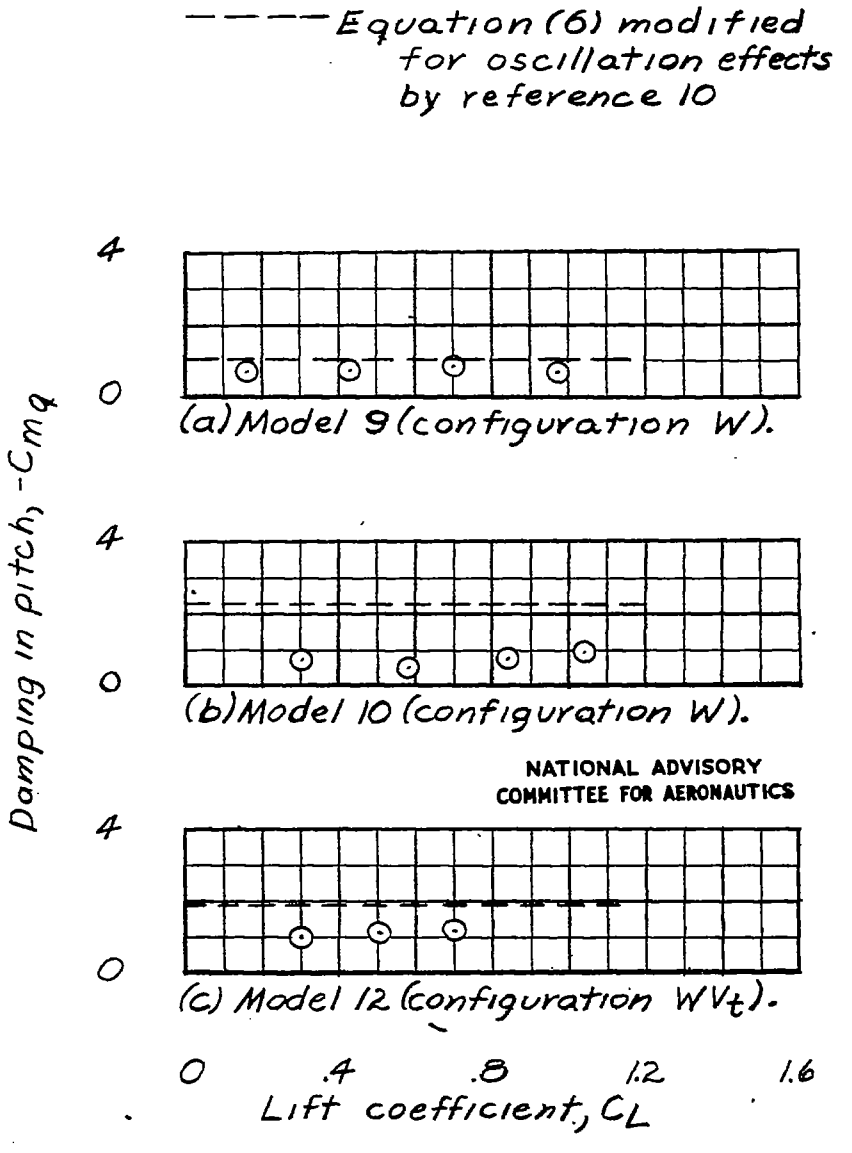

Figure 24.- Effect of lift coefficient on damping in pitch of several tailless models tested in Langley free-flight tunnel. Calculations are for wing alone.

Model	C_L	$\frac{S_H}{S}$	$\frac{l}{b}$	T_c	δ_f (deg)
○	2	0.9	0.206	0.53	0	0
□	2	1.5	.206	.53	1.2	0
◇	2	1.5	.206	.53	0	40
△	2	9	.206	.53	.6	40
▽	2	1.6	.206	.53	1.2	40
▽	6	.4	.080	.35	Prop.off	0
◁	6	.4	.160	.35	Prop.off	0
▷	6	.4	.240	.35	Prop.off	0

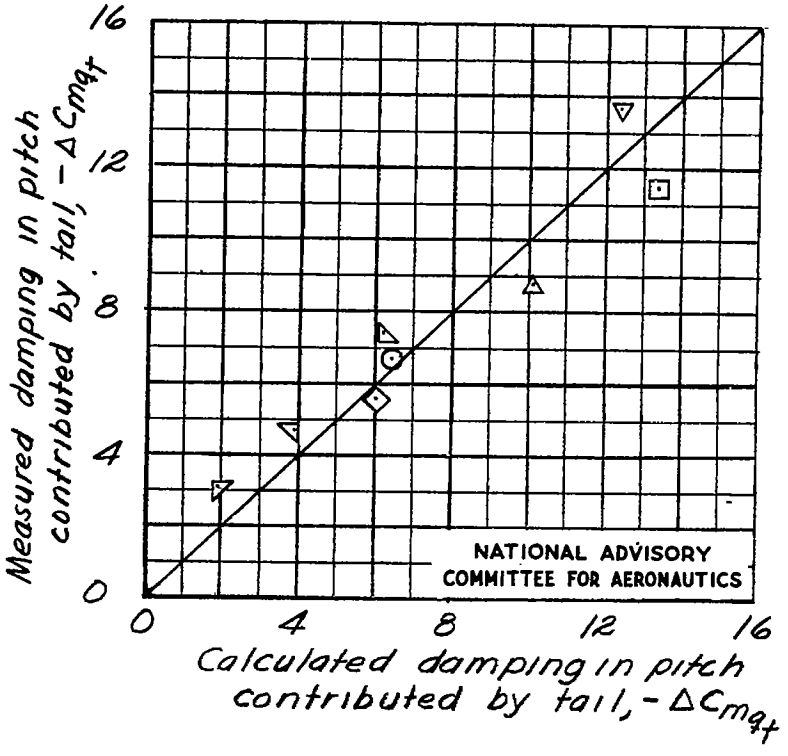

Figure 25.-Comparison of measured damping in pitch contributed by horizontal tail with calculated values from equation (7).

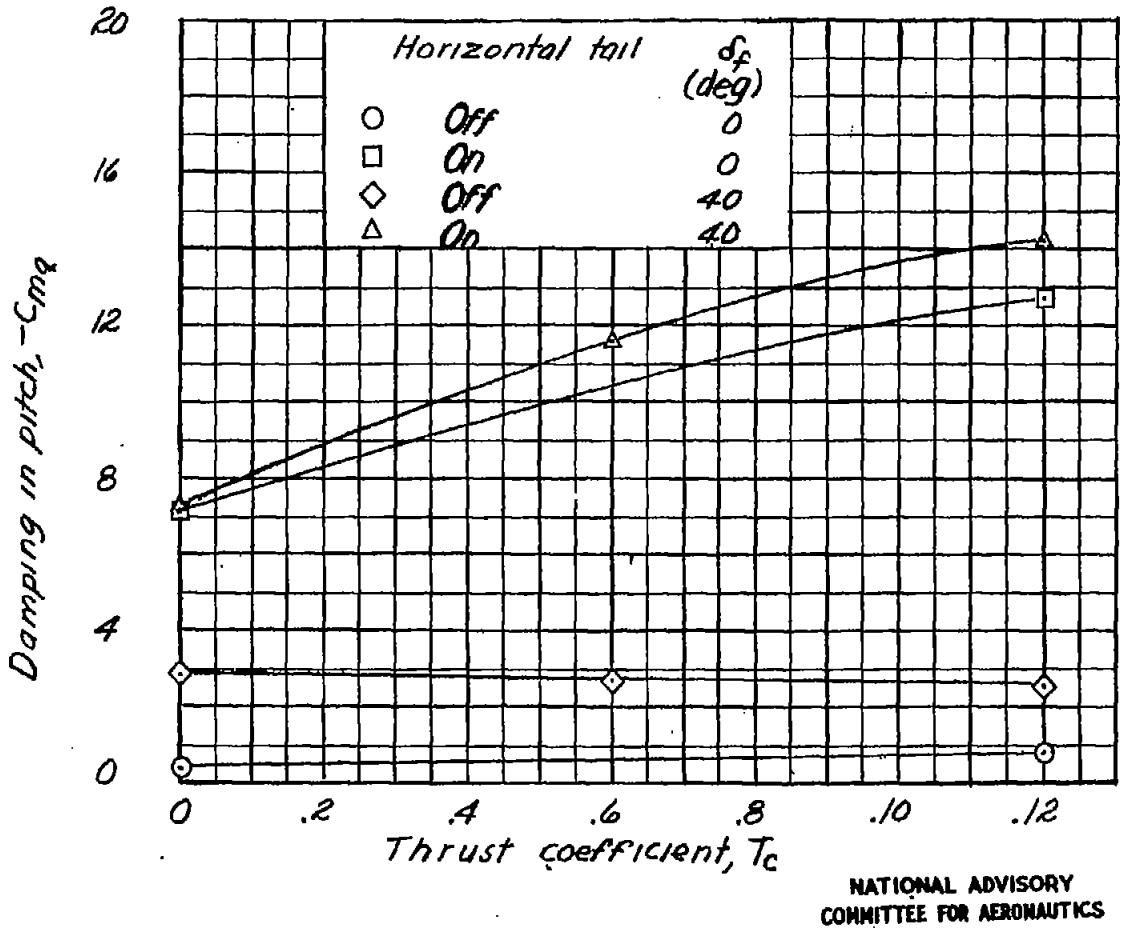

Figure 26.- Effect of thrust coefficient on damping in pitch of model 2. $C_L = 0.9$; $\frac{S_H}{S} = 0.206$; $\frac{l}{b} = 0.63$.